

# Neural Entropy

Akhil Premkumar

*Kavli Institute for Cosmological Physics, University of Chicago, IL 60637, USA*

## Abstract

We examine the connection between deep learning and information theory through the paradigm of diffusion models. Using well-established principles from non-equilibrium thermodynamics we can characterize the amount of information required to reverse a diffusive process. Neural networks store this information and operate in a manner reminiscent of Maxwell’s demon during the generative stage. We illustrate this cycle using a novel diffusion scheme we call the entropy matching model, wherein the information conveyed to the network during training exactly corresponds to the entropy that must be negated during reversal. We demonstrate that this entropy can be used to analyze the encoding efficiency and storage capacity of the network. This conceptual picture blends elements of stochastic optimal control, thermodynamics, information theory, and optimal transport, and raises the prospect of applying diffusion models as a test bench to understand neural networks.

# Contents

<b>1</b>	<b>Introduction</b>	<b>3</b>
<b>2</b>	<b>A Generalized Bound</b>	<b>6</b>
<b>3</b>	<b>Dissipation, Lag, and the Information Gap</b>	<b>8</b>
<b>4</b>	<b>The Diffusion Demon</b>	<b>10</b>
<b>5</b>	<b>Score Matching</b>	<b>13</b>
<b>6</b>	<b>Entropy Matching</b>	<b>14</b>
<b>7</b>	<b>Experiments</b>	<b>17</b>
<b>8</b>	<b>Conclusions</b>	<b>22</b>
<b>A</b>	<b>Information Theory and Statistical Mechanics</b>	<b>26</b>
A.1	The Maximum Entropy Principle . . . . .	26
A.2	Entropy Production in Stochastic Processes . . . . .	29
<b>B</b>	<b>Supporting Calculations</b>	<b>31</b>
B.1	Derivation of the Bound . . . . .	31
B.2	The $H$ -theorem . . . . .	34
B.3	Denoising Objective . . . . .	35
	<b>References</b>	<b>38</b>

# 1 Introduction

In many ways recent advances in the field of machine learning parallel the development of thermodynamics in the 19<sup>th</sup> century. Much like the mechanical engines of that era, machine learning algorithms have made epochal progress in solving problems of great practical importance. However, at the heart of these algorithms is a component we do not yet fully understand: neural networks. A full effective theory of neural networks is still forthcoming, but they possess one feature that is unambiguous and nearly universal—these are systems with a large number of degrees of freedom that collectively exhibit emergent behavior.

Boltzmann’s pioneering work on statistical mechanics was conceived under similar circumstances, when the existence of atoms was still not widely accepted. In particular, the atomistic viewpoint reveals how the Second Law of Thermodynamics emerges from the statistics of large numbers [1]. In time, these ideas would reappear with greater generality under the guise of Shannon’s Information Theory [2]. The fundamental relationship between thermodynamics and information theory would be revealed later, through the resolution of a decades-old thought experiment featuring Maxwell’s demon [3], whose namesake spurred Boltzmann’s research in the first place.

In this paper we explore whether ideas from thermodynamics and information theory can be used to understand the behavior of neural networks. Diffusion models serve as a natural bridge to draw the connection between thermodynamics and machine learning, because they were originally developed by synthesizing ideas from these disciplines [4]. Very briefly, samples from a training dataset are incrementally noised till they are distributed as a generic Gaussian, while a neural network learns to reverse these noising steps. Once trained, the network can transform a random Gaussian vector into a highly structured output that resembles a typical member of the training data. In the continuum limit, the noising and denoising stages become diffusive processes [5], the thermodynamic properties of which are well established. A neural network embedded within the diffusion paradigm must follow the rules of thermodynamics, specifically the Second Law—as the model creates structure out of noise in one part of the system, it must simultaneously produce disorder in others. This disorder is held as information in the neural network, in a manner that evokes Maxwell’s demon, allowing us to quantify the information with a property we refer to as *neural entropy*.

Diffusion gradually wipes out information from the system over time, but the process can be reversed by reinstating the lost information. In a diffusion model the neural network stores this information. Entropy is a measure of ‘missing information’ (see App. A), so the total entropy produced during the forward process also quantifies the amount of information the network needs to remember and put back during reversal

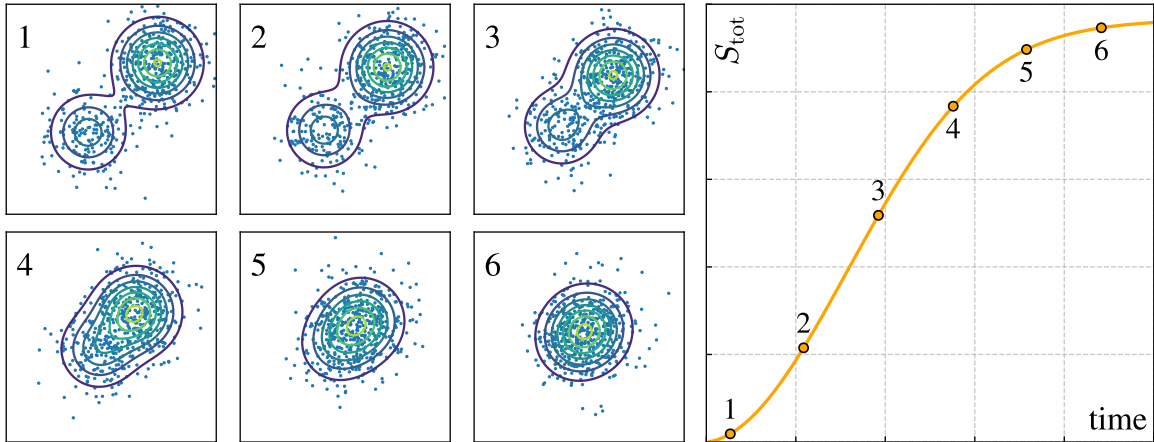


Figure 1: Diffusion is a non-equilibrium process that generates entropy over time. On the left we see snapshots of a diffusive process (Ornstein-Uhlenbeck). In the forward direction the distribution evolves from  $1 \rightarrow 6$ , and entropy produced till that point in time is indicated on the right. In the reverse direction,  $6 \rightarrow 1$ , a diffusion model removes this excess entropy using information it learned during training. Note that  $S_{\text{tot}}$  is the total entropy produced, which is different from the change in Gibbs entropy of the distribution (see App. A.2).

(see Fig. 1). This is the central idea that leads to the concept of neural entropy.

The entropic point of view can be demonstrated with a reparameterization of the reverse diffusion process from the popular denoising score matching formulation [6]. We call this the *entropy matching model*. The neural entropy of this model is the total dissipation in the forward diffusion process, which has a lower bound related to the  $L^2$ -Wasserstein distance between the initial data distribution and the final Gaussian [7]. Thus we establish a fundamental connection between diffusion models and the theory of optimal transport, opening up a new space of design choices for future diffusion models. Furthermore, diffusion models are infinitely deep variational autoencoders [8], therefore neural entropy offers a way to characterize a neural network’s performance as an encoder.

**Outline:** A brief summary of each section is given below, highlighting the key ideas discussed therein.

- Sec. 2: We develop a generalized upper bound on the KL divergence between the data and generated distributions in a diffusion model (cf. Eq. (2.6)).
- Sec. 3: For a special case, the bound can be understood as a Jarzynski equality for diffusion (cf. Eq. (3.1)). The forward diffusive process adds information to

the system, increasing its entropy. Reversal must remove this excess entropy.

- **Sec. 4:** Knowing 1 bit of information about a system allows us to lower its entropy by  $\log 2$ . When we train a diffusion model we deliver to a neural network an amount of information equivalent to the entropy produced in the forward transformation. We call this neural entropy.
- **Sec. 5** The neural entropy of a score matching model has anomalous properties that make it less useful as a measure of the information stored in the network.
- **Sec. 6:** The entropy matching model is introduced, the neural entropy of which is precisely the thermodynamic entropy produced by diffusion. The connection between diffusion models and optimal transport is made more transparent through entropy matching (cf. Eq. (6.5)).
- **Sec. 7:** By computing the KL divergence between the data and generated distributions we can get a sense of the neural network performance for different values of neural entropy. See Fig. 6. The training loss is correlated with the information the network fails to absorb. It could potentially be used as a measure of network performance when the KL is not calculable (cf. Fig. 9).
- **App. A:** Statistical mechanics presented as a form of statistical inference, with Shannon entropy as a measure of information. The relation to nonequilibrium processes is also discussed.
- **App. B:** A mathematical supplement with detailed derivations of the results in the main text.

**Notation:** We use the time variable  $s$  for the forward diffusion process, which runs from right ( $s = 0$ ) to left ( $s = T$ ) in Fig. 2. Sometimes we indicate functions of  $s$  as  $\overleftarrow{f}$  to remove ambiguity when the same function is also expressed in terms of time variable  $t = T - s$ . That is,  $\overleftarrow{f}(s) = \overleftarrow{f}(T - t) = f(t)$ .  $\hat{B}_s$  and  $B_t$  denote the Brownian motions associated with the forward and reverse/controlled SDEs, respectively.  $\nabla$  is the gradient with respect the spatial coordinates, and  $\partial_t, \partial_s$  are partial time derivatives.  $S_{\text{tot}}$  is the total entropy produced during forward diffusion,  $S_G$  is the non-equilibrium Gibbs entropy of the distribution, and  $S_{\text{NN}}$  is the neural entropy. Throughout the paper, we set Boltzmann’s constant to unity,  $k_B = 1$ .  $\log$  is the natural logarithm.  $p_d$  and  $p_0$  denote the initial ( $s = 0$ ) and final ( $s = T$ ) densities for the forward process.  $p_u(\cdot, 0)$  and  $p_u(\cdot, T)$  are the initial ( $t = 0$ ) and final ( $t = T$ ) densities of the controlled process. There is a slight abuse of notation here because  $p_u(\cdot, 0)$  is a prior that does not depend on the control  $u$ .

## 2 A Generalized Bound

Given a set of data vectors, probabilistic models attempt to learn the underlying data distribution from which these vectors could have been sampled. One way to do this is to minimize the KL divergence between the data and the model distributions. Score-based diffusion models are trained by optimizing an objective that upper bounds this KL [9, 8]. In this section, we extend this bound to a more general parameterization of the generative process. This will allow us to interpret the upper bound as an entropy later in the paper.

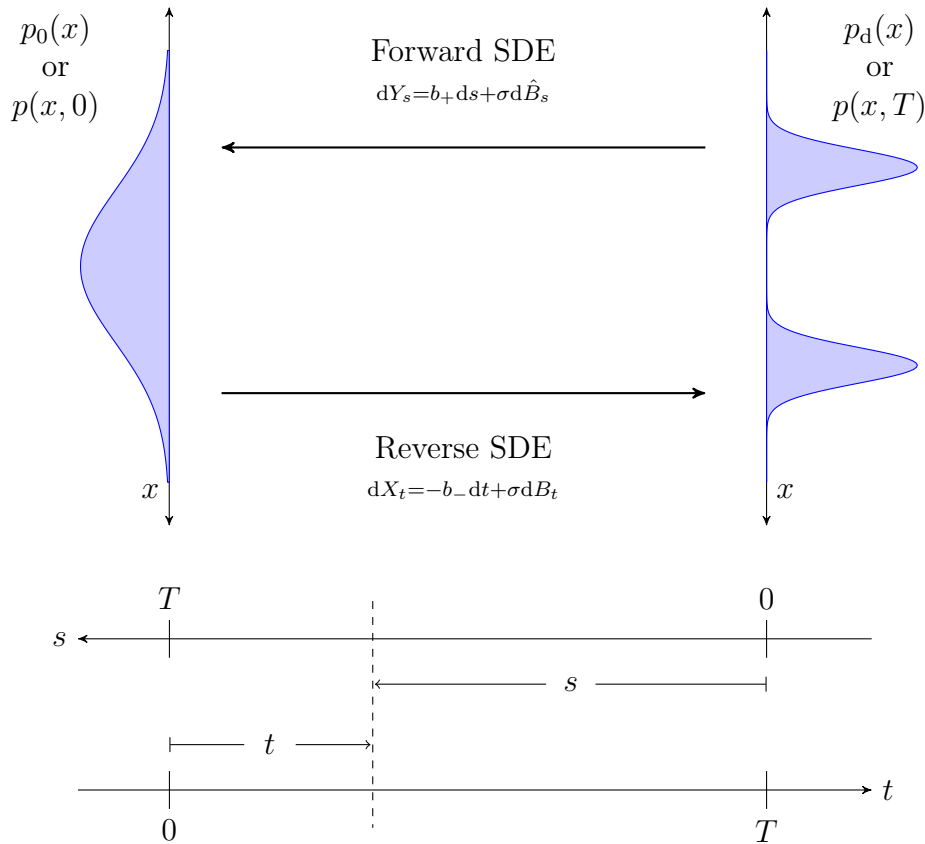


Figure 2: A schematic of the forward and reverse diffusion processes.

Consider a  $D$ -dimensional probability density function  $p_d$  subjected to a diffusive process

$$dY = b_+(Y, s)ds + \sigma(s)d\hat{B}_s. \quad (2.1)$$

The noise is isotropic and position-independent. Under Eq. (2.1), the distribution  $p_d(y) \equiv \overleftarrow{p}(y, 0)$  evolves to some another distribution  $p_0(y) \equiv \overleftarrow{p}(y, T)$  (see Fig. 2). This

process can be reversed by an SDE [10, 11, 12, 13]

$$dX = -b_-(X, T-t)dt + \sigma(T-t)dB_t, \quad (2.2)$$

where  $t = T - s$ , and the drift term is

$$b_-(X, s) = b_+(X, s) - \sigma^2(s)\nabla \log \overleftarrow{p}(X, s). \quad (2.3)$$

Starting from  $p_0(x) \equiv p(x, 0)$ , the reverse evolution back to  $p_d(x) \equiv p(x, T)$  appears as a playback of the forward process in Eq. (2.1), so that  $p(x, t) = \overleftarrow{p}(x, T-t)$  at an intermediate time  $t$ . Crucially, we need information about the forward process, specifically the *score function*  $\nabla \log \overleftarrow{p}$ , to construct the reverse drift term in Eq. (2.3). This makes sense: the final distribution  $p_0$  has little to no memory of the initial state  $p_d$ , meaning that many different  $p_d$  could diffuse to roughly the same  $p_0$ , rendering the problem non-invertible without explicit knowledge of the forward process.

If we replace  $b_-$  in Eq. (2.2) with a different drift term  $u$ , which we call the *control*, and evolve  $p_0(x)$  by the stochastic process

$$dX = -u(X, t)dt + \sigma(T-t)dB_t, \quad (2.4)$$

the density  $p_u(x, t)$  of  $X_t$  will differ from  $p(x, t)$ , and land on a terminal distribution  $p_u(x, T) \neq p(x, T)$ . The Kullback-Leibler divergence between these distributions is bounded as<sup>1</sup>

$$\int_0^T dt \frac{1}{2\sigma^2} \mathbb{E}_p [\|b_- - u\|^2] \geq D_{KL}(p(\cdot, T) \| p_u(\cdot, T)). \quad (2.5)$$

More generally, if we start at some  $p_u(x, 0) \neq p_0(x)$ ,

$$\int_0^T dt \frac{1}{2\sigma^2} \mathbb{E}_p [\|b_- - u\|^2] + D_{KL}(p_0(\cdot) \| p_u(\cdot, 0)) \geq D_{KL}(p(\cdot, T) \| p_u(\cdot, T)). \quad (2.6)$$

This result can be derived using the theory of stochastic optimal control [15], or by an application of the Feynman-Kac formula and Girsanov's theorem [8, 16]. The details are relegated to App. B.1.

As a particular example we can choose  $u = b_+ - \sigma^2 \mathbf{s}_\theta$ , where  $\mathbf{s}_\theta$  is the output of a neural network, which converts the l.h.s. in Eq. (2.5) into the score-matching objective from [6, 5]. This leads to Theorem 1 from [9],

$$\int_0^T dt \frac{\sigma^2}{2} \mathbb{E}_p [\|\mathbf{s}_\theta - \nabla \log p\|^2] + D_{KL}(p_0 \| p_{u0}) \geq D_{KL}(p(\cdot, T) \| p_u(\cdot, T)). \quad (2.7)$$

---

<sup>1</sup>The expectation value in Eq. (2.5),  $\int dt \mathbb{E}_p \equiv \int dt \mathbb{E}_{p(\cdot, t)}$ , is a *path integral* [14].

If we pick a  $p_{u0}$  close to  $p_0$ , and train a neural network to minimize the score-matching term, we can tighten the KL divergence between the data distribution and the generated one. This is how diffusion models work. More generally, Eq. (2.5) has a strong likeness to an important relation in thermodynamics called the *Jarzynski equality*, specifically the form given in Eq. (40) of [17]. This expression relates the total entropy production to the KL divergence between probability distributions of forward and reverse trajectories [18]. Eq. (2.5) can be understood along the same lines.

### 3 Dissipation, Lag, and the Information Gap

To draw the connection to thermodynamics, let us choose  $u = -b_+$  in Eq. (2.4), and assume that  $p_{0u} = p_0$ . Then,

$$S_{\text{tot}}(T) := \int_0^T dt \frac{1}{2\sigma^2} \mathbb{E}_p \left[ \|2b_+ - \sigma^2 \nabla \log p\|^2 \right] \geq D_{KL}(p(\cdot, T) \| p_{-b_+}(\cdot, T)). \quad (3.1)$$

The l.h.s. is the total entropy produced as the distribution  $p_d$  is diffused to  $p_0$  by Eq. (2.1) [19]. As diffusion progresses, our knowledge of the system diminishes over time.  $S_{\text{tot}}$  is a measure of this information loss.<sup>2</sup> To undo diffusion we must restore the information worn away in the forward process. We can sharpen this intuition by analyzing Eq. (3.1) in greater detail.

As it stands, Eq. (3.1) resembles the Vaikuntanathan-Jarzynski (VJ) relation for irreversible processes [20], namely

$$W_{\text{diss}}(t) \geq \beta^{-1} D_{KL}(\rho_t \| \rho_t^{\text{eq}}). \quad (3.2)$$

This relation can be understood by considering a system, initially at a temperature  $\beta^{-1}$ , driven away from equilibrium by varying an external parameter  $\lambda$  from  $A$  to  $B$ , over a time interval  $t \in [0, T]$ . Let  $\langle W \rangle$  be the average mechanical work needed to affect this transformation, which is at least equal to the free energy difference  $\Delta F$  between  $A$  and  $B$ . This is the Second Law. Then,  $W_{\text{diss}} = \langle W \rangle - \Delta F$  is the average work dissipated over the whole process.  $\rho_t$  is the phase space density as the system evolves from  $A$  to  $B$ , and  $\rho_t^{\text{eq}}$  is the equilibrium density corresponding to the value of the parameter at that instant,  $\lambda_t$ .<sup>3</sup> That is, if we adjust the parameter to  $\lambda_t$  and wait a long time, the system will evolve to  $\rho_t^{\text{eq}}$ , its entropy increasing monotonically during the process. This is Boltzmann's  $H$ -theorem [1, 15]. In other words  $\rho_t^{\text{eq}}$  is the maximum entropy distribution consistent with  $\lambda_t$  [21, 22].

<sup>2</sup>For  $b_+ \neq 0$ ,  $S_{\text{tot}}$  is not simply the difference in *Gibbs* entropy between  $p_d$  and  $p_0$  (see App. A.2).

<sup>3</sup> $\rho_t^{\text{eq}} \equiv \rho^{\text{eq}}(\cdot, \lambda_t)$  depends on time only through the parameter  $\lambda_t$ .



On the other hand, under finite time non-equilibrium evolution the system is rushed along to the state  $\rho_t$ , and is not afforded the time to relax to the maximum entropy configuration. As a result, a *lag* develops between  $\rho_t$  and  $\rho_t^{\text{eq}}$ , as measured by the KL divergence in Eq. (3.2). Lag indicates the extent to which the system is out of equilibrium. The VJ relation, Eq. (3.2), says that the dissipated work dictates the maximum extent to which the equilibrium can be broken at a given instant.

We can also interpret the lag as the *information gap* between  $\rho_t$  and  $\rho_t^{\text{eq}}$ . The entropy of a system is a measure of missing information, with larger entropy associated with a greater degree of ignorance about the system's true state (see App. A).  $\rho_t^{\text{eq}}$  has a higher entropy than  $\rho_t$ , since much of the information in the latter is lost when  $\rho_t$  equilibrates to  $\rho_t^{\text{eq}}$ . Intuitively, it is clear that the gap is precisely the amount of information we need to exhume  $\rho_t$  from  $\rho_t^{\text{eq}}$ .

In the context of Eq. (3.1), the non-equilibrium process is the reverse diffusion from Eq. (2.2). The KL divergence in Eq. (3.1) can be thought of as a kind of lag that develops between the probability distributions, as  $p_0$  is evolved to  $p$  and  $p_{-b_+}$  respectively by (see footnote 3)

$$dX = -b_-(X, T-t)dt + \sigma(T-t)dB_t, \quad (3.3a)$$

$$dX = b_+(X, T-t)dt + \sigma(T-t)dB_t. \quad (3.3b)$$

However,  $D_{KL}(p||p_{-b_+})$  is not quite the lag from Eq. (3.2) because  $p_{-b_+}$  is not the equilibrium distribution corresponding to Eq. (3.3b). In fact, such a distribution must solve the homogeneous Fokker-Planck equation (see footnote 3)

$$\partial_t p_t^{\text{eq}} = 0 = -\nabla \cdot (b_+ p_t^{\text{eq}}) + \frac{\sigma^2}{2} \nabla^2 p_t^{\text{eq}} \implies p_t^{\text{eq}} \propto \exp \left[ \int dx \frac{2b_+}{\sigma^2} \right]. \quad (3.4)$$

The solution  $p_t^{\text{eq}}$  is called a *quasi-invariant* distribution [16], and it corresponds to the maximum entropy configuration consistent with the value of  $b_+$  and  $\sigma$  at the instant  $t$  (see App. A.2). It can be shown that replacing  $p_{-b_+}$  with  $p^{\text{eq}}$  saturates Eq. (3.1) (see App. B.2),

$$\int_0^T dt \frac{1}{2\sigma^2} \mathbb{E}_p \left[ \|2b_+ - \sigma^2 \nabla \log p\|^2 \right] + D_{KL}(p_0||p_0^{\text{eq}}) = D_{KL}(p(\cdot, T)||p_T^{\text{eq}}(\cdot)). \quad (3.5)$$

The KL term on the l.h.s. is worth some attention. Recall that  $p_0$  is the result of diffusing  $p_d$  with Eq. (2.1) for a duration  $T$ . Since  $T$  is finite,  $p_0$  still contains remnants of  $p_d$ , unlike  $p_0^{\text{eq}}$  which has no memory of its initial conditions. We can understand the inequality in Eq. (3.1) along similar lines: if we diffuse  $p_d \rightarrow p_0$  and reverse it via Eq. (3.3b),  $p_{-b_+}$  contains traces of  $p$ , which means the information gap between  $p$  and

$p_{-b_+}$  is not quite as large as that between  $p$  and  $p^{\text{eq}}$ .

The VJ relation also forces a shift in perspective, nudging us to think of the controlled evolution Eq. (3.3b) as the ‘natural’ dynamics of the system, with the process in Eq. (3.3a) driving it away from its preferred state  $p_{-b_+}$ . The gap measures the information deficit that keeps the controlled dynamics from reaching  $p_d$  on its own.<sup>4</sup> We can close the gap by modifying the control to supply this additional information. Eq. (3.1) tells us that, starting with  $p_0$  and  $u = -b_+$ , the *maximum* additional information needed to arrive at  $p_d$  is  $S_{\text{tot}}$ .

These arguments also serve to illustrate a specific point about the Second Law: it is a statement about the irreversibility of a non-equilibrium transformation, *even if* that process is simulated on a computer. In the real world irreversibility is an observed property of almost all physical processes<sup>5</sup> [27, 28], but we take this for granted since we evolve with SDEs that are not time-symmetric by construction (cf. Eq. (2.1)).

## 4 The Diffusion Demon

Building on the perspective developed in the previous section and generalizing a bit, we can define an entropy-like quantity

$$S_u(t) := \int_0^t d\bar{t} \frac{1}{2\sigma^2} \mathbb{E}_p [\|b_- - u\|^2]. \quad (4.1)$$

By Eq. (2.6), this is the maximum information gap at time  $t$  between a distribution  $p$  reverse diffusing from  $p_0 \rightarrow p_d$ , and a  $p_u$  generated by evolving  $p_u(\cdot, 0)$  with Eq. (2.4). That is, the control  $u$ , and diffusion coefficient  $\sigma^2$  specify the ‘natural’ dynamics of the system, or equivalently, its quasi-invariant state.  $S_u(t)$  is the maximum lag that develops as we force the system to reverse diffuse to  $p_d$ .

We can parameterize the control as  $u = u_a + u_\theta$ , where  $u_a$  is some analytic expression of  $x$  and  $t$ , and  $u_\theta$  is the output of a neural network with parameters  $\theta$  trained to minimize  $S_u(T)$ . If the network is disconnected, the gap between the reverse and controlled distributions will be bounded as

$$\int_0^T dt \frac{1}{2\sigma^2} \mathbb{E}_p [\|b_- - u_a\|^2] \geq D_{KL}(p(\cdot, T) \| p_{u_a}(\cdot, T)) - D_{KL}(p(\cdot, 0) \| p_u(\cdot, 0)). \quad (4.2)$$

The l.h.s. is the information stored in the network during the forward process (training),

---

<sup>4</sup>This way of framing the problem echoes a classic *gedankenexperiment* due to Schrödinger [23, 24].

<sup>5</sup>We are specifically referring to systems with a large number of degrees of freedom,  $N$ ; if  $N$  is small enough it is possible to obtain ‘second law violating’ behavior, see for e.g. [25, 26], and App. A.1.

and the r.h.s. is the excess entropy that must be siphoned away from  $p_{u_a}$  during reversal (generation). This use of previously measured information to alter the entropy of a system is reminiscent of *Maxwell's demon* [3]. The relationship between a diffusion model and Maxwell's demon runs deeper, and warrants further discussion.

Maxwell originally conceived of a *temperature demon* [29], a tiny imaginary being that operates a small door on a partition that separates a chamber into two parts of equal volumes, the left and right. The chamber contains a gas that is initially at equilibrium, i.e. its temperature  $T_0$  is uniform over the entire volume of the chamber. Let  $\langle v \rangle_0$  be the average speed of the gas molecules. The demon observes the molecules moving around the chamber, and if a molecule approaches from the left with a velocity less than  $\langle v \rangle_0$ , he opens the door and lets the molecule go to the right side. If a molecule from the right approaches with a velocity greater than  $\langle v \rangle_0$ , he lets it pass to the left. Once a small temperature difference develops between the right and the left, the demon's action continues to move heat from the colder part (right) to the hotter part (left) without exerting any work. This appears to be a violation of the Second Law; if a fast molecule that passes from right to left carries with it heat  $\delta Q$ , the entropy of the gas changes by  $\delta S = \delta Q/T_{\text{left}} - \delta Q/T_{\text{right}} < 0$ .

The paradox is resolved if we include the demon in our appraisal of entropy. To be able to decide whether an incoming molecule can pass through the door, the demon must remember the current average velocity of one of the chambers. He also needs to keep track of this number in his memory after allowing each molecule to pass through, so he can take the correct action for the next molecule arriving at the door. However, memory is a physical system, the internal state of which changes when information is stored in it. We can eliminate these extraneous degrees of freedom from our entropy calculation by erasing the contents of the demon's memory, thereby restoring it to its original state. Erasing memory is a dissipative process that increases the entropy of its environment—this is Landauer's *erasure principle* [30, 31]. The erasure step releases enough entropy to save the Second Law.

To be clear, measuring and storing information in memory does not raise the 'entropy of the memory' [32]. Rather, the information in the memory is *associated* with the amount of entropy it can negate. Knowing one bit of information about a system allows us to lower its entropy by at most  $\log 2$ . Erasing one bit of information releases at least  $\log 2$  entropy. This is independent of how the memory is implemented in hardware.

In a diffusion model, the neural network performs the role of the demon's memory (see Fig. 3). During the forward process the total entropy increases monotonically, as more and more information is washed away by diffusion. But the model records this information in its network during training, just like how the demon remembers veloc-

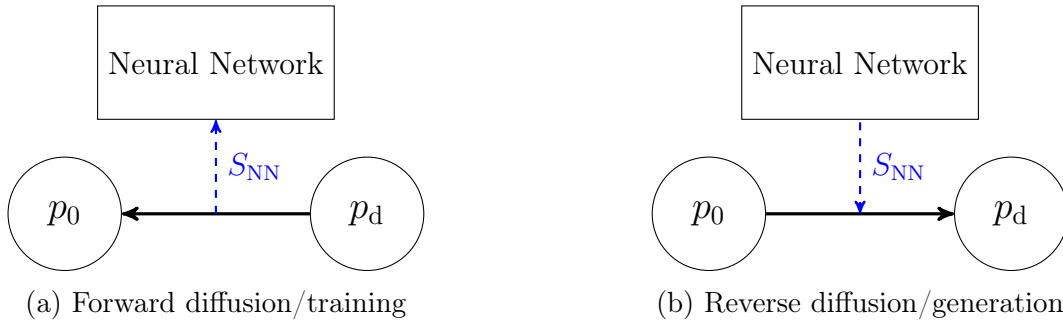


Figure 3: An idealized cycle of a diffusion model. During the forward process information lost as  $p_d$  transforms to  $p_0$  is captured by a neural network. This information is applied to lower the entropy of the system and recover  $p_d$  in the reverse process. The dashed arrow indicates the flow of information.

ities, so the content of the original distribution is not truly lost. We can recover this distribution by re-introducing the stored information back into the system. However, there is a subtle point to note here: in the reverse process the neural network output is applied as a drift term  $u_\theta$ . This is a departure from the demon’s operation of opening and closing the door since the latter does not involve any interaction with the particles. Nonetheless, both actions modify path probabilities in a manner that appears to defy the Second Law.

Consider once again the setup in Eq. (4.2). The diffusing particles prefer the quasi-invariant distribution, which corresponds to the maximum entropy configuration consistent with the value of  $u_a$  and  $\sigma^2$  at that instant. Therefore, any deviation from this state would lower the entropy (see App. A.2). Such a departure can be induced using information about the system from a prior measurement, which for a diffusion model is the training phase. The maximum amount of information delivered to the network during training is  $S_{u_a}(T)$ , which we shall henceforth refer to as *neural entropy*,

$$S_{\text{NN}}(T) := \int_0^T dt \frac{1}{2\sigma^2} \mathbb{E}_p [\|b_- - u_a\|^2]. \quad (4.3)$$

It is important to stress that  $S_{\text{NN}}$  quantifies the information stored in a perfectly trained network; it is *not* the entropy of internal phase space density over the neural network’s microstates. In a diffusion model the network is configured as a memory, and it must be able to retain  $S_{\text{NN}}/\log 2$  bits of information. However, the storage capacity of the network is not simply the bit count of the parameters of the network—depending on how the network encodes information, it works as an *effective memory* that furnishes a functional bit count that is different from the sum of its parts. Nonetheless it is reasonable to expect the former to scale with the latter.

## 5 Score Matching

It is apparent from Eq. (4.3) that the choice of how we split the control to  $u = u_a + u_\theta$  has a strong bearing on the value of neural entropy. Recall that  $S_{\text{NN}}$  is the maximum gap that develops between the reverse and controlled distributions when the network is disconnected,

$$dX = -b_- dt + \sigma dB_t, \quad (5.1a)$$

$$dX = -u_a dt + \sigma dB_t. \quad (5.1b)$$

For example, in the score-matching parameterization  $u = b_+ - \sigma^2 \mathbf{s}_\theta$  (cf. Eq. (2.7)), so  $u_a = b_+$ . This may seem like the natural choice for  $u_a$ , given  $b_- = b_+ - \sigma^2 \nabla \log \overleftarrow{p}$ . However, several factors hamper the adoption of the entropic viewpoint in score matching models. These problems stem from the fact that  $b_+$  is a confining drift term in forward diffusion, which means  $-u_a = -b_+$  is not. Therefore, Eq. (5.1b) does not have a quasi-invariant distribution, and the intuition from Sec. 3 no longer holds. We can identify the inconsistencies arising from this conceptual breakdown through a straightforward calculation.

Starting with Eq. (4.3), let us tentatively define the score matching neural entropy

$$S_{\text{NN}}^{\text{sm}}(T) := \int_0^T dt \frac{\sigma^2}{2} \mathbb{E}_p [\|\nabla \log p\|^2]. \quad (5.2)$$

The quantity on the right can be related to the non-equilibrium Gibbs entropy of the diffusing distribution, which we will write in terms of the time variable  $s$  (cf. Eq. (A.9)). The change in Gibbs entropy under the forward process is (cf. Eq. (A.10))

$$\overleftarrow{S}_{\text{G}}(T) - \overleftarrow{S}_{\text{G}}(0) = \int_0^T ds \mathbb{E}_{\overleftarrow{p}} \left[ \frac{\sigma^2}{2} \left\| \nabla \log \overleftarrow{p} \right\|^2 + \nabla \cdot b_+ \right]. \quad (5.3)$$

We may therefore rewrite Eq. (5.2) as

$$S_{\text{NN}}^{\text{sm}}(T) = \overleftarrow{S}_{\text{G}}(T) - \overleftarrow{S}_{\text{G}}(0) - \int_0^T ds \mathbb{E}_{\overleftarrow{p}} [\nabla \cdot b_+]. \quad (5.4)$$

To simplify further we need to choose the drift term  $b_+$ . A popular choice in diffusion models is the Variance Preserving (VP) process [4, 5], for which  $b_+(y, s) = -\beta(s)y/2$

and  $\sigma(s) = \sqrt{\beta(s)}$  in Eq. (2.1), where  $\beta(s)$  is positive. Then, Eq. (5.4) reduces to<sup>6</sup>

$$S_{\text{NN}}^{\text{VP}}(T) = \overleftarrow{S}_{\text{G}}(T) - \overleftarrow{S}_{\text{G}}(0) + \frac{D}{2} \int_0^T ds \beta(s). \quad (5.5)$$

Upon closer inspection, Eq. (5.5) reveals a problem with the score matching neural entropy. Consider the trivial case where  $p_0$  and  $p_d$  are identical. The Gibbs entropy at the initial and final times are equal, therefore the first two terms cancel. But we are still left with a positive integral on the r.h.s. (see Fig. 4b). This is also apparent from Eq. (5.2)—the score function is static but it is not zero, so the neural entropy is some positive number, and information is delivered to the network. Now imagine changing  $p_d$  to some other distribution  $p_d'$ , with  $p_0$  and the  $\beta$ -schedule kept fixed. The only change in Eq. (4.3) is the  $-\overleftarrow{S}_{\text{G}}(0)$  term. As a result, if  $p_d'$  has a larger entropy than  $p_d$  the neural entropy decreases. It would seem that the network needs to remember *less* information to transform  $p_0 \rightarrow p_d'$  than it does to convert  $p_d$  to itself!

The issue is rooted in the decision to set  $u_a = b_+$ . For the VP process, Eq. (5.1b) is then

$$dX = \frac{\beta}{2} X dt + \sigma dB_t. \quad (5.6)$$

But this SDE has a repulsive drift term which, given enough time, dilutes the distribution away to infinity. Therefore, the network  $u_\theta$  needs to work against  $u_a$  to keep the distribution  $p_u$  intact. In the above examples the growth in neural entropy due to the  $\int ds \beta(s)$  term in Eq. (5.5) is indicative of the information needed to hold the diffusing particles in place as the drift  $\beta X/2$  tries to drive them apart. For this reason the score matching neural entropy from Eq. (5.2) is not an accurate gauge of the non-trivial information the network must store to reverse diffusion.

## 6 Entropy Matching

Motivated by the observations in Sec. 5 we introduce a new model that furnishes a physically sensible neural entropy—if more information is sent to the network, the neural entropy must increase proportionally. The important change is the parameterization of the control as

$$u = -b_+ - \sigma^2 \mathbf{e}_\theta. \quad (6.1)$$

---

<sup>6</sup>Explicitly,  $\nabla \cdot b_+ = -\frac{1}{2}\beta(s)\nabla \cdot x = -\frac{D}{2}\beta(s)$ .

That is,  $u_a = -b_+$ , which makes the neural entropy the same as the total entropy generated during the forward diffusion process (cf. Eq. (3.1)),

$$S_{\text{NN}}^{\text{em}}(T) = \int_0^T dt \frac{1}{2\sigma^2} \mathbb{E}_p \left[ \|2b_+ - \sigma^2 \nabla \log p\|^2 \right] \equiv S_{\text{tot}}. \quad (6.2)$$

The key advantage is that, for a forward process that asymptotes to a stationary distribution as  $s \rightarrow T$ , and the entropy production slows down as diffusion unfolds (see Fig. 1). To see this analytically we start by substituting Eq. (6.1) into Eq. (2.6),

$$\int_0^T ds \frac{\sigma^2}{2} \mathbb{E}_{\overleftarrow{p}} \left[ \left\| \frac{2b_+}{\sigma^2} - \nabla \log \overleftarrow{p} + \mathbf{e}_\theta \right\|^2 \right] + D_{\text{KL}}(p_0(\cdot) \| p_\theta(\cdot, 0)) \geq D_{\text{KL}}(p(\cdot, T) \| p_\theta(\cdot, T)). \quad (6.3)$$

The network is trained to minimize the integral in Eq. (6.3). In practice we do not know  $\nabla \log \overleftarrow{p}$  so we must use a denoising objective in lieu of this term. Furthermore, the time integral and expectation are computed by Monte Carlo (see App. B.3), leading to the *denoising entropy matching loss*:

$$\mathbb{E}_{s \sim \mathcal{U}(0, T)} \left[ \sigma(s)^2 \mathbb{E}_{y_0 \sim p_d(y_0)} \mathbb{E}_{y_s \sim \overleftarrow{p}(y_s | y_0)} \left[ \frac{1}{2} \left\| \frac{2b_+}{\sigma^2} - \nabla \log \overleftarrow{p}(y_s | y_0) + \mathbf{e}_\theta \right\|^2 \right] \right]. \quad (6.4)$$

For instance, if we choose the VP process,  $2b_+/\sigma^2 = -y_s$ . At some time  $s_*$  the distribution  $\overleftarrow{p}$  resembles the final state of the VP process, a Gaussian with zero mean and unit variance along each dimension, as does the transition probability  $\overleftarrow{p}(y_s | y_0)$ . The gradient of the log of the latter is  $\sim -y_s$  so the first two terms inside the norm nearly cancel beyond  $s_*$ , which means  $\mathbf{e}_\theta \sim 0$ , and no further information is pushed to the network (see Fig. 4). Had we started with  $p_d \sim p_0$ , very little neural entropy would have been produced, which makes perfect sense.

The entropy  $S_{\text{NN}}^{\text{em}}(T)$  by itself does not tell us anything about *how* the network stores the information. A diffusion model is an infinitely deep variational autoencoder [8]. Internally, the model tries to encode  $S_{\text{NN}}^{\text{em}}(T)$  worth of information in some clever way, but it is only partially successful. The non-zero loss function at the end of training reflects information ‘leakage’, that is, the portion of  $S_{\text{NN}}^{\text{em}}(T)$  that the network fails to absorb. Up to some additive constants, the loss function from Eq. (6.4) upper bounds the KL divergence between the data and generated distributions,  $p_d(\cdot)$  and  $p_\theta(\cdot, T)$  (cf. Eqs. (6.3) and (B.23)).<sup>7</sup> The true measure of the model’s performance is this KL, which is what we use in our experiments in Sec. 7 to assess the network’s retention

<sup>7</sup>In practice, there is also a multiplicative pre-factor introduced into Eq. (6.4) which has been empirically found to improve the model performance [6, 9].

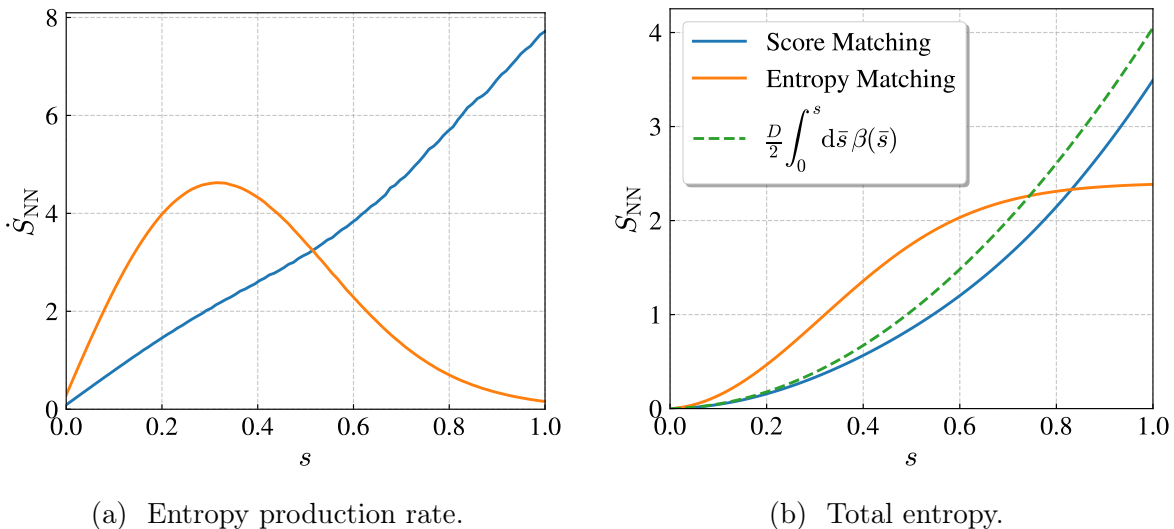


Figure 4: Neural entropy over time for score matching and entropy matching models with a VP process. For the latter the neural entropy is the same as  $S_{\text{tot}}$  (cf. Eqs. (3.1) and (6.2)), which is why entropy production trails off as forward diffusion approaches its final state.

of  $S_{\text{NN}}^{\text{em}}(T)$ . In this way, the KL vs. neural entropy curves serve as a *coarse* diagnostic of the storage and encoding capacity of the network. The relation between these two quantities is not always a one-to-one map, as we will see in Sec. 7.

The entropy matching model also draws an important connection between diffusion models, thermodynamics, and optimal transport. This link is established through the *Benamou-Brenier formula* [7], which can be used to relate the entropy produced in a diffusive process with the  $L^2$ -Wasserstein distance between  $p_0$  and  $p_d$  [33]. For the diffusion process Eq. (2.1),

$$\min_{b_+} S_{\text{tot}} = \frac{\mathcal{W}_2(p_d, p_0)^2}{2\sigma^2 T}, \quad (6.5)$$

with the diffusion coefficient  $\sigma^2$  set to a constant. Taken together, Eqs. (6.2) and (6.5) show that the neural network needs to retain very little information if  $p_d$  and  $p_0$  are close to one another in the  $\mathcal{W}_2$  sense, which is eminently reasonable. An experimental demonstration of this fact is given in Fig. 8a. Furthermore, there is some optimal choice of the drift  $b_+$  for a given pair  $(p_d, p_0)$  that brings the neural entropy close to its minimum possible value.<sup>8</sup> These observations open up a new space of design choices for diffusion models where we choose  $p_0$  and the parameters of the forward process to

<sup>8</sup>A relationship between the score matching objective and a Wasserstein distance is also established in [34], but their expressions involve  $\mathcal{W}_2$  between distributions at the same instants of time, for e.g.  $\mathcal{W}_2(p(\cdot, T), p_u(\cdot, T))$ .



optimize the entropic load on the neural network. Specifically, Eq. (6.5) signals that we ought to be cognizant of thermodynamic speed limits when choosing the drift and diffusion coefficients [35]. These considerations will be explored in future work.

## 7 Experiments

Neural entropy, as defined in Eq. (4.3), measures the maximum information content presented to the network in an idealized setting. However, in practice we face two broad limitations:

1. **Imperfect data:** We only have access to  $p_d$  through its samples. The number and quality of these samples strongly affect the quality of the reconstructed distribution.
2. **Imperfect learning:** The training process is stochastic by design and we never truly make the loss function zero. Since the neural entropy is simply the loss function with the network disconnected, the residual loss indicates that not all of the information has been absorbed by the network.

To address point 1 we will work with synthetic datasets sampled from simple multivariate distributions  $p_d$  for which we have closed form expressions (for e.g. Gaussian mixtures). This allows us to produce as many samples as we require with high fidelity, and know the exact likelihood of each of those samples. We can also work in arbitrary dimensions. With regard to point 2, recall from Eq. (2.6) that the loss function upper bounds the KL divergence between the data distribution, and the generated distribution,  $D_{KL}(p_d(\cdot) \| p_\theta(\cdot, T))$ , which means this KL can be used to assess the performance of the diffusion model—a larger residual loss would mean a higher KL. For any sample  $x$  we know  $p_d(x)$  and  $\log p_d(x)$ , so all we need to compute the KL is  $\log p_\theta(x, T)$ . We have developed a method to do this, which will be elaborated on in an upcoming paper.

We also investigated how neural entropy evolves over time. For very low dimensional distributions ( $D = 2$ , say) the analytic expressions for  $\nabla \log \overleftarrow{p}$  can be plugged into Eqs. (5.2) and (6.2) and integrated numerically to compute the respective neural entropies. Through our experiments we found that the corresponding expressions computed with just the neural network output agree extremely well with the actual analytic curves. That is,

$$S_\theta(T) := \int_0^T ds \frac{\sigma^2}{2} \mathbb{E}_{\overleftarrow{p}} [\|\mathbf{n}_\theta\|^2], \quad \mathbf{n}_\theta = \begin{cases} \mathbf{s}_\theta, & \text{score matching,} \\ \mathbf{e}_\theta, & \text{entropy matching.} \end{cases} \quad (7.1)$$

is a good approximation to the true  $S_{\text{NN}}^{\text{sm}}$  and  $S_{\text{NN}}^{\text{em}}$ , and is much easier to compute in higher dimensions. In our experiments we estimate Eq. (7.1) by Monte Carlo (see for e.g. Eq. (B.27)). When we discuss neural entropy in this section we are talking about the corresponding  $S_{\theta}(T)$ .

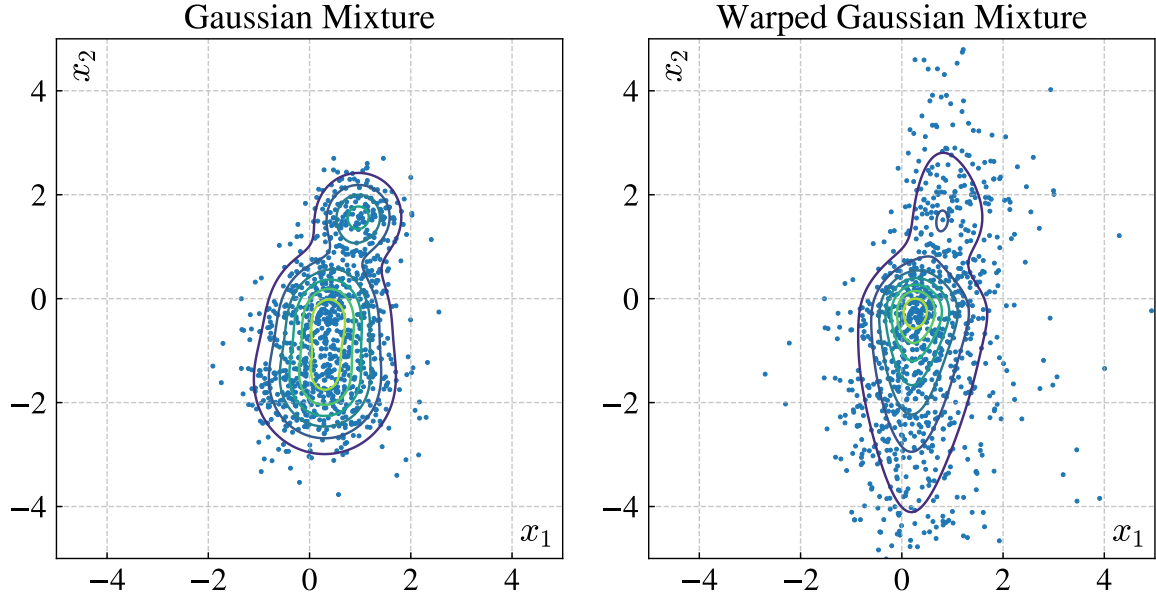


Figure 5: A representative example of the kind of  $p_d$  distributions we use in our experiments. These are distributions in  $D = 2$  dimensions but the actual distributions we use live in  $D = 4$  to  $8$  dimensions. The diffusion models are trained on samples from these  $p_d$ , indicated by the blue dots. The warped densities are created with Eq. (7.2).

Our experiments are designed to test how a neural network responds to different amounts of information, as characterized by the neural entropy  $S_{\text{NN}}^{\text{em}}$ . The latter is a function of  $p_d, p_0$ , and the forward process, Eq. (2.1). We vary  $S_{\text{NN}}^{\text{em}}$  by changing  $p_d$ , whilst keeping  $p_0, b_+$ , and  $\sigma$  fixed. We work with two kinds of  $p_d$ , Gaussian mixtures and coordinate transformed versions of Gaussian mixtures (see Fig. 5). These are low dimensional distributions, typically  $D = 4$  to  $8$ , and our network is a simple MLP with Gaussian random feature layers for  $x$  and  $t$  [36]. The structure of the network is *kept fixed* in all the experiments, so its capacity to store information is the same in all cases. The diffusion model is trained on data sampled from  $p_d$ . These sample are noised by a VP process [5], with  $\beta_{\min} = 0.1$  and  $\beta_{\max} = 8$ . Then, we compute  $D_{KL}(p_d(\cdot) || p_{\theta}(\cdot, T))$  on a new set of samples from  $p_d$ . The main output of our experiments are plots of this KL against  $S_{\text{NN}}^{\text{em}}$  (see Fig. 6). There is a clear deterioration in the network performance as we try to push more information into it.

As we argued in Sec. 5, the neural entropy for score matching models trends in

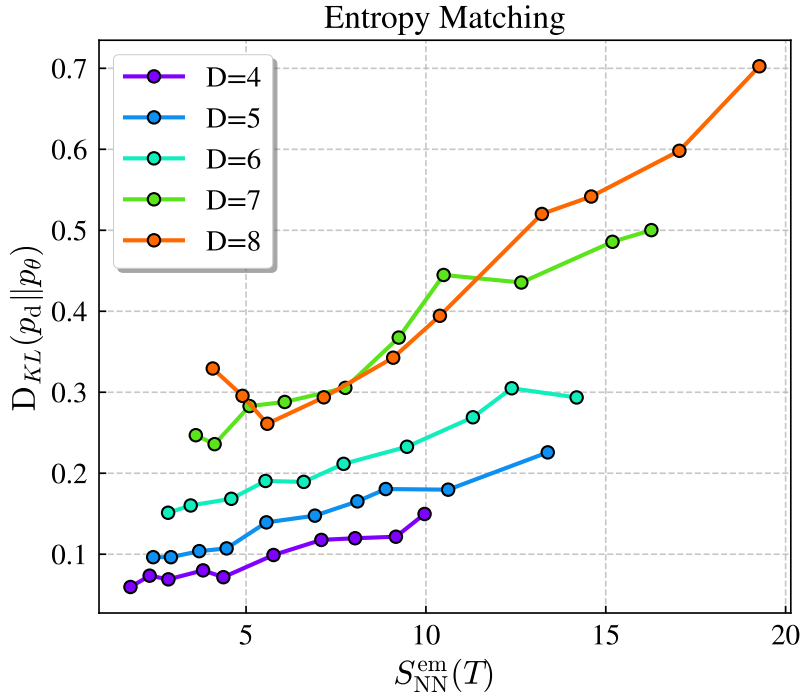


Figure 6: Plots of the KL divergence between the data distribution  $p_d(\cdot)$  and the generated distribution  $p_\theta(\cdot, T)$  against the neural entropy delivered in an entropy matching model. Each point corresponds to a  $p_d$  distribution associated with a different neural entropy. In this plot the  $p_d$ 's are randomly generated Gaussian mixtures in  $D$  dimensions. Lower values of the KL indicate better performance of the diffusion model. Pushing more information into the neural network deteriorates model performance.

a manner that is at odds with our natural notion of entropy production (see Sec. 3). Nonetheless, we carried out experiments to study KL vs.  $S_{\text{NN}}^{\text{sm}}$  as well (see Fig. 7). These curves demonstrate the anomalous behavior of  $S_{\text{NN}}^{\text{sm}}$ —a lower value of this entropy gives higher KL, which we take to mean that the network had to retain more information. However, it is worth noting that the overall performance of the score matching model consistently exceeds that of the entropy matching model, given the same  $p_0, p_d$ , and diffusion parameters. This needs to be studied in detail.

A neural network is just a collection of weights and biases connected in some specific way. These hyperparameters are stored as real bits on a computer. It is reasonable to wonder if the quantity we identify as neural entropy is simply counting the number of these real bits used to store the information needed for reversal.<sup>9</sup> The form of Eq. (7.1) supports such speculation since it can be understood as an aggregate of all the ‘snapshots’ of the total entropy or score the network remembers, up to a factor  $\sigma^2/2$ .

<sup>9</sup>We thank Lorenzo Orecchia for discussions related to this point.

That is, if the  $\mathbf{n}_\theta$  were small almost everywhere, the network stores little information, the hyperparameters are nearly zero, and  $S_\theta$  would be low. On the other hand, if  $\mathbf{n}_\theta$  were large, the hyperparameters would also be larger numbers stored over more real bits in the computer’s memory, and  $S_\theta$  would be high. However, the experiments with the score matching model discredit this point of view—smaller values of  $S_\theta$  give poorer KL in those models (with  $\sigma$ -schedule fixed), demonstrating that the actual information the network must encode is different from the raw magnitudes of the snapshots presented to the network.

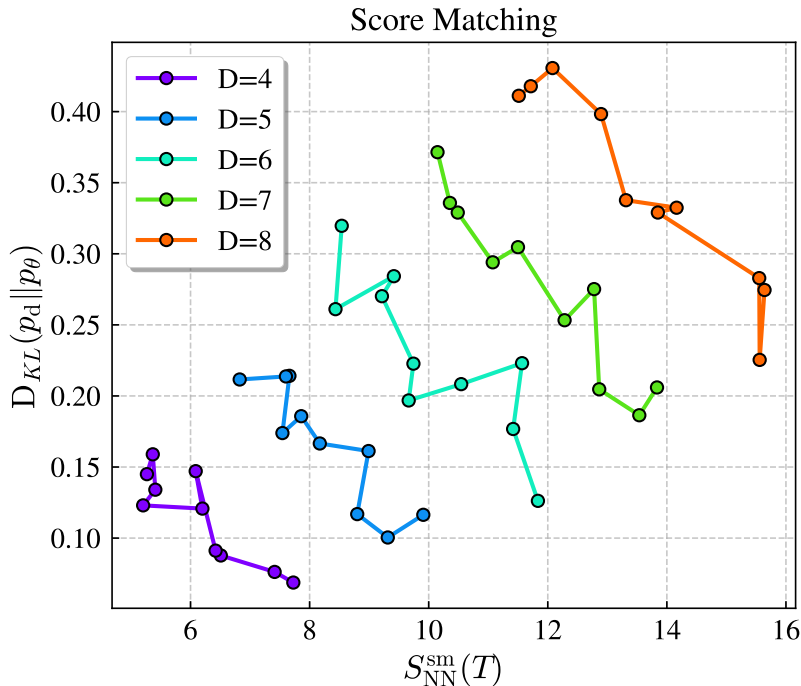


Figure 7: KL vs. neural entropy for the score matching model. The network performance decreases at lower values of entropy, in contrast to the trend in Fig. 6. This behavior is explained in Sec. 5.

Our diffusion model can work with arbitrary data distributions. To add a little variety to the  $p_d$ ’s we take a Gaussian mixture and ‘warp’ it with a co-ordinate transformation

$$\tilde{x} = \sinh(\gamma x), \quad (7.2)$$

where  $\gamma$  is a number we vary from 0.1 to 0.9. Under any smooth invertible transformation  $\tilde{X} = g(X)$ , the Gibbs entropy of the  $X$ -distribution changes to

$$\check{S}_G = S_G + \mathbb{E}_X \left[ \log \left| \frac{\partial g(x)}{\partial x} \right| \right]. \quad (7.3)$$

The sinh transformation is interesting because it stretches or compresses the distribution according to the choice of  $\gamma$ , allowing us to produce non-trivial  $p_d$ 's that are not simply scaled versions of one another (see Fig. 5). Consequently, the neural entropy associated with these warped distributions changes non-linearly with  $\gamma$ . The KL response to these entropies are shown in Fig. 8.

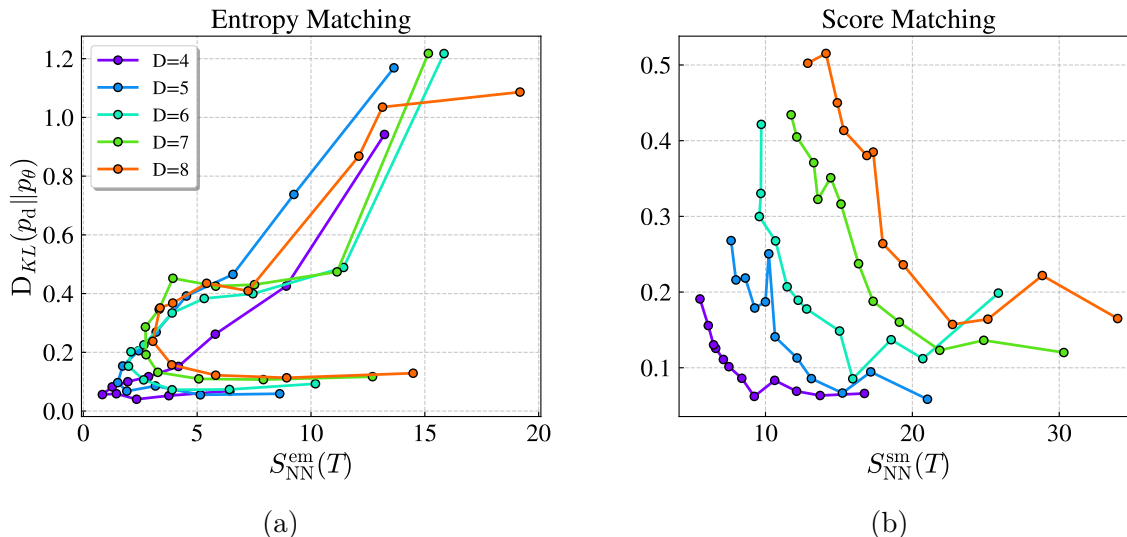


Figure 8: KL vs. neural entropy for the warped Gaussian mixtures.

The ‘C’ shape of the plots in Fig. 8a are particularly noteworthy. We use a VP process in our experiments, for which  $p_0$  is a standard normal Gaussian, for any distribution  $p_d$ . The warped  $p_d$  for  $\gamma = 0.1$  is smaller than  $p_0$  and grows in size as  $\gamma$  is increased. The entropy of the transformation,  $S_{NN}^{em}(T) \equiv S_{tot}$ , is smallest around  $\gamma = 0.4$ , which is when  $p_d$  has roughly the same size as  $p_0$ . Increasing  $\gamma$  further makes  $p_d$  grow larger, causing the neural entropy to rise. This behavior demonstrates the connection to optimal transport made in Eq. (6.5)—the total entropy produced is lower if  $p_d$  and  $p_0$  are close to one another in the  $\mathcal{W}_2$  sense. This concordance is absent in Fig. 8b, which further illustrates how the entropy matching model is better suited for characterizing the neural network performance.

Two more points need to be made about Fig. 8a: (1) It shows that the relation between the KL and  $S_{NN}^{em}$  is not one-to-one; two different data distributions that produce the same  $S_{NN}^{em}$  are encoded differently in the network. Therefore, neural entropy alone does not determine model performance. (2) There is nothing special about the transformation in Eq. (7.2). We could have obtained the ‘C’ curves using Gaussian mixtures that increased in size in a similar way; for the experiments in Figs. 6 and 7 all  $p_d$  were larger than the standard normal distribution  $p_0$ .

Finally, we study the training loss as a function of the neural entropy for both

models. All our models are trained for 200 epochs, which is well beyond the point where the losses settle to their final value. Fig. 9 shows the final value of loss against neural entropy. Observe how the trends are correlated with the KL plots in Figs. 6, 7 and 8a. This correlation arises because the loss is proportional to the upper bound on the KL divergence between the data distribution and the generated one (cf. Eq. (2.6)). It also suggests that *loss could be used as a proxy for entropy retention in the network*, in those cases where the KL divergence is difficult to compute (for instance, when  $p_d$  is not known).

## 8 Conclusions

We have introduced the idea of neural entropy and demonstrated that, with entropy matching diffusion models, it can be used to quantify the information delivered to a neural network. We then gauge the network’s effectiveness at encoding and storing this information by how well it reconstructs the data distribution. This paradigm serves as a test bench for neural network architectures, which may be used to assess their performance against different kinds of data and training parameters.

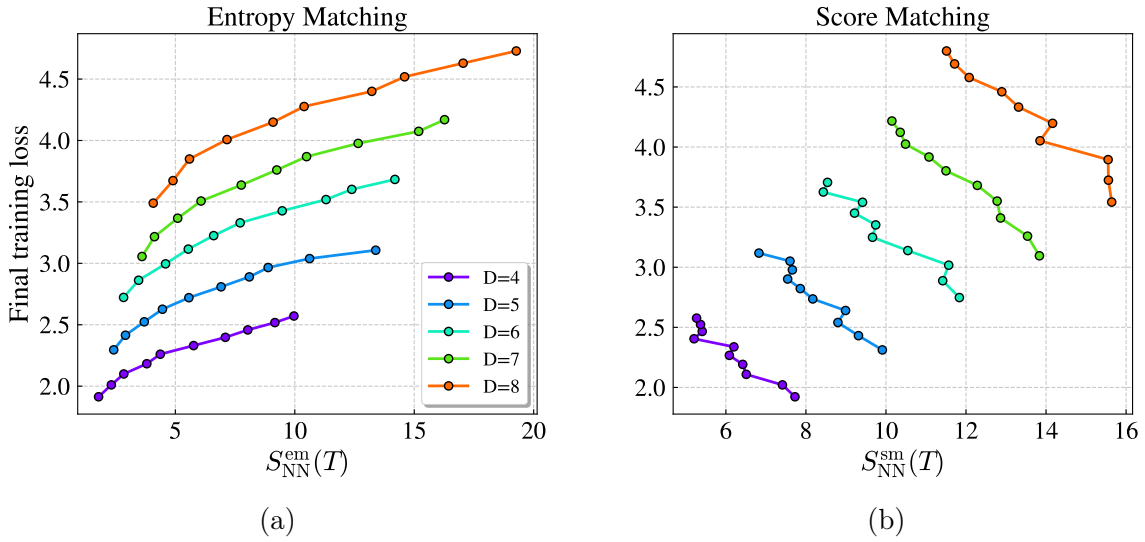
The experiments in this paper are simple proof of concepts that provide a blueprint for more sophisticated probes of neural network and/or diffusion model performance. We highlight a few ideas worth exploring in the immediate future:

1. The entropy matching model offers a precise connection between diffusion models and optimal transport. Given the same  $p_d$  and  $p_0$ , there exists some way of diffusing  $p_d \rightarrow p_0$  that incurs minimum entropy production. This helps constrain the forward diffusion coefficients, for e.g. the  $\beta$ -schedule for VP processes.
2. We can use neural entropy to understand the role of symmetries in learning. Neural entropy, and the associated KL divergence characterize the data space and say nothing of the hyperparameters inside the network. However, there is an intimate relationship between the two. In particular if the data distribution possesses some symmetries, an equivariant neural network constructed from the ground up to respect those symmetries would be able to encode  $S_{\text{NN}}^{\text{em}}$  more efficiently. Therefore it is reasonable to expect a noticeable improvement in KL performance of such a network vis-à-vis a regular non-equivariant network, for finite batch size and training epochs.<sup>10</sup>
3. The neural entropy test bench is agnostic to the nature of the diffusion model’s memory. In our experiments we used a simple MLP, but we can swap it out

---

<sup>10</sup>We thank Maurice Weiler for pointing this out.

With Gaussian mixture data distributions



With warped Gaussian mixture distributions

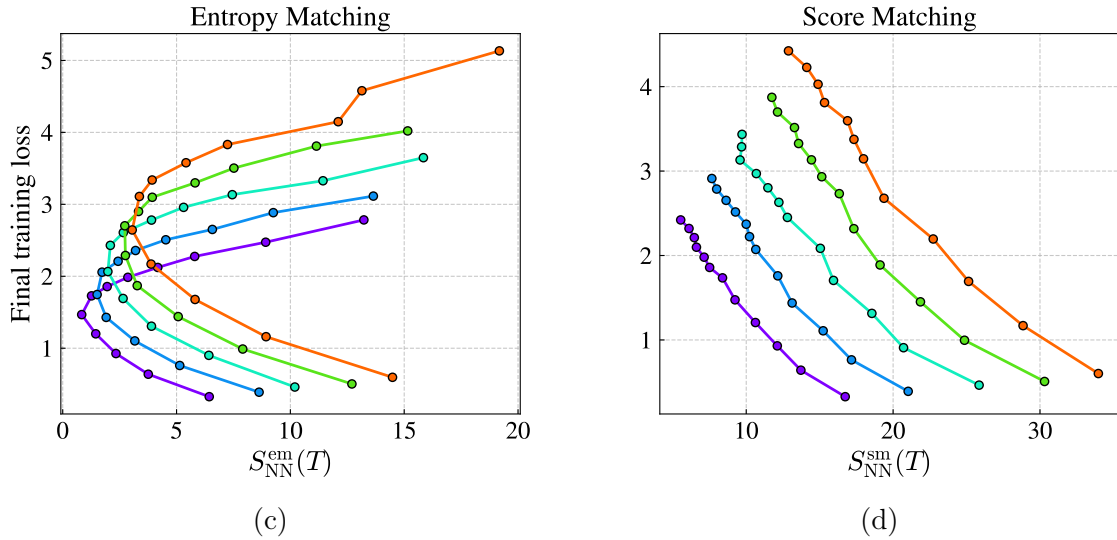


Figure 9: The final training loss at the end of 200 epochs, plotted against the neural entropy in entropy matching and score matching models. Loss grows with neural entropy in Fig. 9a, which is the sensible behavior, but it shows the opposite trend for score matching models, in Fig. 9b. A similar behavior is observed in Fig. 9d. In particular, Fig. 9c demonstrates that the same value of the total entropy can give rise to different losses. Note how the losses track the behavior of the KL divergences in Figs. 6, 7 and 8a. This is a consequence of Eq. (2.6).

with a U-net or even a transformer [37] to study how they perform with practical data sets. In such cases the training loss would be a more reasonable metric to evaluate the model since the KL is likely too difficult to compute (see Fig. 9). The neural entropy can be estimated from the network output using Eq. (7.1).

## Related Work

This work draws ideas from several papers that came before, and it is worth comparing and contrasting our contributions in relation to some of them.

**Variational perspective and stochastic control:** The fundamental relationship at the heart of this paper, Eq. (2.6), was derived by combining ideas from [15, 8]. The stochastic control approach in [15] was applied to generative modeling in [38, 39]. The methods in [8] also appear in [16, 40], which derive a Jarzynski equality for the diffusion process using the Feynman-Kac formula and Girsanov’s theorem.

**Thermodynamics:** The connection between entropy production and path probabilities along forward and reverse schedules was pioneered through the works of Jarzynski and Crooks [25, 41]. The literature on this subject is far too extensive to cite faithfully here, but we found the results most pertinent to diffusive processes are summarized in [14]. The particular version of the Jarzynski equality we use in our work is from [20], which relates dissipation to the loss of equilibrium in an irreversible process. A slightly different perspective is given in [42], which connects dissipation to the time-reversal asymmetry of such a process. This viewpoint is closer to the original inspiration for diffusion models [4].

**Optimal transport:** As this work was in final preparation, [35] appeared, where the authors used the thermodynamic speed limit [33] to study the trade-off between speed and accuracy in diffusion models. We touched on this idea in Sec. 6, where we pointed out that the entropy matching model makes the connection to optimal transport much more obvious. The relation between score matching and optimal transport is discussed in [34].

**Neural density estimation:** In our experiments we compute the KL divergence between the data distribution and the generated one. This is made possible by a technique we developed to estimate log likelihoods from the diffusion model. This approach will be presented in an upcoming paper, at which time the code for this work will also be made available. The current method for exact likelihood computation



involves converting the reverse diffusion SDE into an ODE, which can be solved for  $\log p$  [5]. This process is too slow however, because solving the ODE is a sequential operation. Our approach is much faster.

## Acknowledgements

We thank Lorenzo Orecchia, William Cottrell, Antares Chen, Austin Joyce, and Maurice Weiler for valuable discussions, and Yuji Hirono for bringing [35] to our attention. We are especially grateful to William Cottrell and Lorenzo Orecchia for their comments on the manuscript. The author was supported in part by the Kavli Institute for Cosmological Physics at the University of Chicago through an endowment from the Kavli Foundation. Computational resources for this project were made available through the AI+Science research funding from the Data Science Institute at the University of Chicago.

# A Information Theory and Statistical Mechanics

This complement is meant as a bare-bones review of statistical mechanics for those readers not familiar with the subject, or need a quick refresher. We follow the illuminating paper by Jaynes [21], which starts with entropy as the primitive concept and develops statistical mechanics as a form of statistical inference. This makes the connection to Information Theory quite transparent. The main ideas are demonstrated with a toy example involving dice.

## A.1 The Maximum Entropy Principle

Consider the following problem from [21]: A discrete random variable  $x$  can assume the values  $x_i (i = 1, \dots, n)$ . We are not given the corresponding probabilities  $p_i$ ; all we know is the average value of the function  $f(x)$ ,

$$\langle f(x) \rangle = \sum_{i=1}^n p_i f(x_i). \quad (\text{A.1})$$

Using this information, what is the expectation value of some other function  $g(x)$ ? This appears to be an ill-defined problem since, in addition to Eq. (A.1) and the normalization condition

$$\sum_{i=1}^n p_i = 1, \quad (\text{A.2})$$

we would need  $(n - 2)$  more conditions to determine  $\langle g(x) \rangle$ . The resolution to this problem is to choose the least biased estimate on the given information, so that we avoid incorporating any information beyond what is given in Eq. (A.1). This is accomplished by finding a  $p_i$  that *maximizes the Shannon entropy*

$$H(p_1, \dots, p_n) = -K \sum_{i=1}^n p_i \log p_i \quad (\text{A.3})$$

subject to the constraints Eqs. (A.1) and (A.2) ( $K$  is a positive constant). We can do this by introducing Lagrange multipliers. The resulting  $p_i$  has the form of a Boltzmann distribution,

$$p_i = \frac{e^{-\beta f(x_i)}}{Z}, \quad (\text{A.4})$$

where

$$Z = \sum_{i=1}^n e^{-\beta f(x_i)}, \quad (\text{A.5a})$$

$$\langle f(x) \rangle = -\frac{\partial}{\partial \beta} \log Z. \quad (\text{A.5b})$$

Take, for instance, a six-sided die with the numbers  $i = 1, \dots, 6$ . Suppose we are told that this die throws an average  $\langle i \rangle = \sum_i i p_i$ . From Eq. (A.5),

$$Z_1 = \sum_{i=1}^6 e^{-\beta i} = e^{-\frac{7}{2}\beta} \frac{\sinh(3\beta)}{\sinh(\frac{\beta}{2})}, \quad (\text{A.6a})$$

$$\langle i \rangle = -\frac{\partial}{\partial \beta} \log Z_1 = \frac{7}{2} - 3 \coth(3\beta) + \frac{1}{2} \coth\left(\frac{\beta}{2}\right). \quad (\text{A.6b})$$

Given  $\langle i \rangle$  we can solve Eq. (A.6b) for  $\beta$ , which determines  $p_i = e^{-\beta i}/Z$ . The maximum entropy distributions for a few different values of  $\langle i \rangle$  are shown in Fig. 10. Different values of  $\langle i \rangle$  offer us varying degrees of insight. For instance, being told that  $\langle i \rangle$  is 1 or 6 would dispel any mystery about the die—these can be the average outcome only when the die is loaded to land on those faces alone—so the entropy is zero. At the other extreme, we learn no additional information if the given value of  $\langle i \rangle$  is 3.5, and we can do no better than assume that all faces are equally likely.

But why would the maximum entropy distribution give a sensible result for  $\langle g(x) \rangle$ ? The answer is that when a large number of degrees of freedom are involved the probability distribution over the collective becomes sharply peaked, with almost all probability concentrated under it. This is the Law of Large Numbers. It is straightforward to see this from our example by computing the statistics of throwing  $N$  dice. The partition function is

$$Z_N = \sum_{\{i_k\}} \prod_{k=1}^N e^{-\beta i_k} = \prod_{k=1}^N \sum_{i_k=1}^6 e^{-\beta i_k} = Z_1^N, \quad (\text{A.7})$$

where the ‘microstates’  $\{i_k\} \equiv \{i_1, \dots, i_N\}$  are the tuple of outcomes for one throw of the  $N$  dice. Denoting the total outcome as  $I := \sum_{k=1}^N i_k$ , we can calculate its expectation value and variance from  $Z_N$ :

$$\langle I \rangle = -\frac{\partial}{\partial \beta} \log Z_N = N \langle i \rangle, \quad (\text{A.8a})$$

$$\text{var}(I) = \langle I^2 \rangle - \langle I \rangle^2 = \frac{\partial^2}{\partial \beta^2} \log Z_N = -N \frac{\partial}{\partial \beta} \langle i \rangle. \quad (\text{A.8b})$$

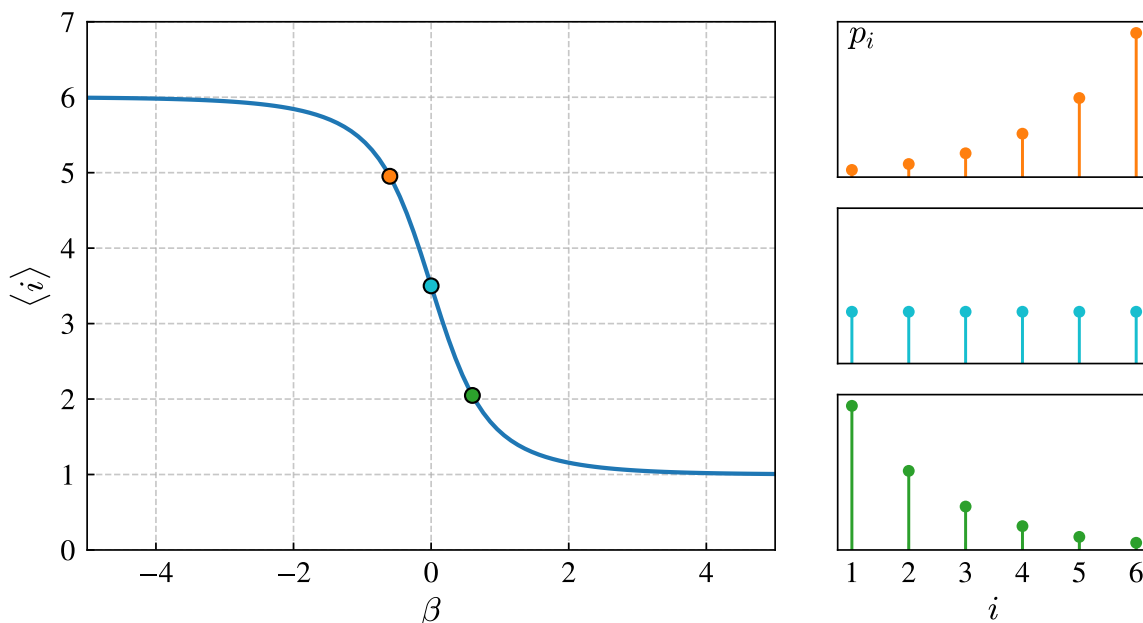


Figure 10: Average result from throwing six-sided die, with the maximum entropy distribution of outcomes for three specific values of  $\langle i \rangle$  shown on the right.

Therefore, the mean of  $I$  scales as  $N$  whereas its standard deviation grows only as  $\sqrt{N}$ . The relative error,  $\sqrt{\text{var}(I)}/\langle I \rangle$  vanishes as  $1/\sqrt{N}$ . Fig. 11 illustrates this behavior. The actual  $p_i$  of the dice is  $p_1 = 0.5, p_2 = p_3 = 0.25$ , and  $p_{i>3} = 0$ , so  $\langle i \rangle = 1.75$ . The maximum entropy distribution corresponding to this  $\langle i \rangle$  is different, it yields almost the same  $P(I)$  in the large  $N$  limit. Notice how the actual dice are incapable of throwing a value larger than 3, whereas the maximum entropy assumption allows this. The difference manifests at the tails of the distribution  $P(I)$ .

The dice experiment demonstrates usefulness of the maximum entropy principle; it prescribes a unique  $p_i$  when there is not enough information to determine the true  $p_i$ . By maximizing Shannon entropy we chose to be maximally noncommittal with regard to the missing information. Those details are *irrelevant* in the large  $N$  limit, since their influence is mostly beaten down by the Law of Large Numbers. So our ambivalence with respect to the missing information is justified. The caveat is that we must restrict ourselves to  $g(x)$  that are insensitive to rare fluctuations, lest they be affected by the the differences between the true and assumed  $p_i$ , even at large  $N$ . For e.g. the maximum entropy predictions for  $\langle e^I \rangle$  will be different from its true value since the exponential is dominated by tail events. See [17, 26, 43, 44] for examples from physics.

The conceptual picture presented here should evoke memories of renormalization

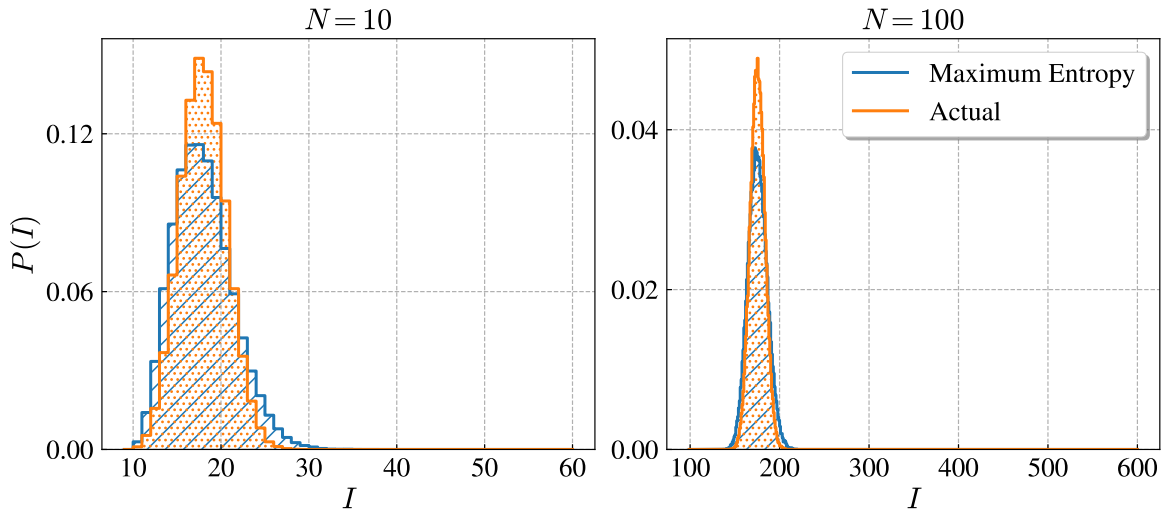


Figure 11: The probability distribution of the total outcome of throwing  $N$  dice, computed by numerical simulation. The actual  $p_i$  of the dice is different from the maximum entropy  $p_i$ , but for large  $N$  both of them yield nearly the same  $P(I)$ .

group theory (RG). The connection is explored in greater detail in [44]. It has also been demonstrated that exact RG can be understood as a diffusive process [45, 46]. For the present work the key takeaway from this section is the idea that Shannon entropy quantifies our lack of knowledge.

## A.2 Entropy Production in Stochastic Processes

Shannon entropy can be understood as a measure of ignorance—by maximizing Eq. (A.3) we are feigning maximal ignorance over the unknowns in the problem. The analogous quantity we use for diffusive processes is the non-equilibrium Gibbs entropy

$$\overleftarrow{S}_G(s) := - \int dx \overleftarrow{p}(x, s) \log \overleftarrow{p}(x, s). \quad (\text{A.9})$$

$\overleftarrow{S}_G$  can be understood as a continuous version of the Shannon entropy,<sup>11</sup> up to a multiplicative factor  $k_B$  which we set to 1 (see footnote 15 in [21]). Gibbs entropy is a measure of our uncertainty in the state of the system, which in this case are the locations of the diffusing particles. But we can choose the drift and diffusion coefficients such that the final distribution is narrower than the initial one (see Fig. 1). Then, our ignorance of the particle positions would be reduced, so the change in Gibbs entropy

<sup>11</sup>Eq. (A.9) is actually the *differential entropy* of a continuous random variable, which has some important differences from the discrete version. Refer chapter 8 of [47] for details.

is *negative*. However, the total entropy increases, as expected, because  $S_{\text{tot}}$  is not just the change in Gibbs entropy.

We can see this explicitly by looking at the expressions for both. Combining Eq. (A.9) with Eq. (B.15) and integrating by parts one obtains

$$\overleftarrow{S}_{\text{G}}(T) - \overleftarrow{S}_{\text{G}}(0) = \int_0^T ds \mathbb{E}_{\overleftarrow{p}} \left[ \frac{\sigma^2}{2} \left\| \nabla \log \overleftarrow{p} \right\|^2 + \nabla \cdot b_+ \right]. \quad (\text{A.10})$$

This is different from the total entropy,

$$S_{\text{tot}} = \int_0^T ds \frac{1}{2\sigma^2} \mathbb{E}_{\overleftarrow{p}} \left[ \left\| 2b_+ - \sigma^2 \nabla \log \overleftarrow{p} \right\|^2 \right]. \quad (\text{A.11})$$

These expressions differ when  $b_+ \neq 0$ . The discrepancy can be understood by looking at the process in the  $t$ -direction. Once again we imagine that the control is being modified to supply the requisite information to convert  $p_0 \rightarrow p_d$ . Recall the following statements from Secs. 3 and 4:

1. Eq. (3.1) tells us that, starting with  $p_0$  and  $u = -b_+$ , the *maximum* additional information needed to arrive at  $p_d$  is  $S_{\text{tot}}$ .
2. Knowing one bit of information about a system allows us to lower its entropy by *at most*  $\log 2$ .

The second point highlights that the actual entropy reduced is only  $\log 2$  for an equilibrium transformation [29]. But diffusion is a nonequilibrium process due to the noise term, which means not all of the information applied translates to a change in the Gibbs entropy. The first point states that  $S_{\text{tot}}$  is the maximum information we need to provide *after* accounting for the component lost to the out-of-equilibrium nature of the transformation. In fact, the Gibbs entropy could even be increasing (along  $t$ ) as we inject information back into the system, under the circumstances described above.

The literature on stochastic thermodynamics accounts for the mismatch by factoring in an additional dissipation due to the mechanical force times displacement [19]. As noise fights the drift term it raises the entropy by

$$\int_0^T ds \frac{1}{2\sigma^2} \mathbb{E}_{\overleftarrow{p}} [b_+ \cdot \dot{y}]. \quad (\text{A.12})$$

A careful calculation reveals that Eq. (A.12) is the difference between Eq. (A.11) and Eq. (A.10) [14]. It can be interpreted as the increase in entropy due to heat dissipated in the medium. In the present context it is sufficient to recognize that  $S_{\text{tot}}$  is the full measure of our ignorance at the end of diffusion.

## B Supporting Calculations

### B.1 Derivation of the Bound

We present a derivation of the bound in Eq. (2.5), drawing from the proofs in [8, 15]. We only outline the steps here, and refer the reader to those papers for more formal details. Consider the process specified by the SDE

$$dX = v(X, t)dt + \sigma(T - t)dB_t \quad (\text{B.1})$$

with the initial condition  $X_0 \sim p_v(\cdot, 0)$ . The evolution of  $p_v(x, t)$  under Eq. (B.1) is given by the Fokker-Planck equation

$$\partial_t p_v + \nabla \cdot (v p_v) - \frac{\sigma^2}{2} \nabla^2 p_v = 0. \quad (\text{B.2})$$

Switching the time variable to  $s = T - t$  (see Fig. 2) converts this into a backward Kolmogorov equation for  $\overleftarrow{p}_v(\cdot, s) := p_v(\cdot, t)$ ,

$$\partial_s \overleftarrow{p}_v - (\nabla \cdot v) \overleftarrow{p}_v - v \cdot \nabla \overleftarrow{p}_v + \frac{\sigma^2}{2} \nabla^2 \overleftarrow{p}_v = 0, \quad (\text{B.3})$$

with the terminal condition  $\overleftarrow{p}_v(\cdot, T) = p_v(\cdot, 0)$ . The solution for Eq. (B.3) is given by the *Feynman-Kac formula*,

$$\overleftarrow{p}_v(x, s) = \mathbb{E} \left[ \overleftarrow{p}_v(Y_T, T) \exp \left( - \int_s^T d\bar{s} \nabla \cdot v(Y_{\bar{s}}, T - \bar{s}) \right) \middle| Y_s = x \right], \quad (\text{B.4})$$

where  $Y_{\bar{s}}$  is a diffusion process that solves

$$dY = -v(Y, T - s)ds + \sigma(s)dB'_s. \quad (\text{B.5})$$

That is, Eq. (B.4) is a *path integral* over all paths that start from  $x$  at time  $s$  and evolve under Eq. (B.5). Setting  $s = 0$  in Eq. (B.4) gives us the likelihood  $p_v(\cdot, T) \equiv \overleftarrow{p}_v(\cdot, 0)$ . Next, [8] bounds the log likelihood by a change of measure and Jensen's inequality,

$$\log p_v(x, T) \geq \mathbb{E}_{\mathbb{Q}} \left[ \frac{d\mathbb{P}}{d\mathbb{Q}} + \log p_v(Y_T, 0) - \int_0^T d\bar{s} \nabla \cdot v \middle| Y_0 = x \right]. \quad (\text{B.6})$$

Here  $\frac{d\mathbb{P}}{d\mathbb{Q}}$  is the Radon-Nikodym derivative. For our purposes it is enough to understand the expectation value of this object as

$$\mathbb{E}_{\mathbb{Q}} \left[ \frac{d\mathbb{P}}{d\mathbb{Q}} \middle| Y_0 = x \right] = - \int dy_T Q(y_T|x) \log \frac{Q(y_T|x)}{P(y_T|x)}, \quad (\text{B.7})$$

where  $P$  is the transition probability corresponding to Eq. (B.5) and  $Q$  is the transition probability for a new process<sup>12</sup>

$$dY = w(Y, s)ds + \sigma(s)d\hat{B}_s. \quad (\text{B.8})$$

Then, Eq. (B.7) can be simplified [24], allowing the r.h.s. in Eq. (B.6) to be written as a cost functional (at  $s = T$ )

$$\overleftarrow{J}(x, s; v, w) := \mathbb{E}_w \left[ \int_s^T d\bar{s} \left( \frac{1}{2\sigma^2} \|v + w\|^2 + \nabla \cdot v \right) - \log p_v(Y_T, 0) \middle| Y_s = x \right]. \quad (\text{B.9})$$

We have tinkered with the notation a little, using  $\mathbb{E}_w$  to indicate that the averages are taken over Eq. (B.8). Eqs. (B.6) and (B.9) will be used in two different ways below. We will set  $p_v(\cdot, 0) = p_0(\cdot)$  in both cases for simplicity.

**Case 1:**  $v = -u$ ,  $w = b_+$ . Then, Eq. (B.1) becomes the controlled process Eq. (2.4) and Eq. (B.8) is the forward diffusion from Eq. (2.1), and Eq. (B.9) is

$$\log p_u(x, T) \geq -\overleftarrow{J}(x, 0; -u, b_+). \quad (\text{B.10})$$

**Case 2:**  $v = -b_-$ . Under this choice Eq. (B.1) is the reverse diffusion process from Eq. (2.2), which takes  $p_0 \rightarrow p_d$  via  $p$ . Then,

$$\log p(x, T) \geq -\overleftarrow{J}(x, 0; -b_-, w). \quad (\text{B.11})$$

This inequality is saturated if we set  $w = b_+$  [15]. To see this, we define the *value function*  $\overleftarrow{W}(x, s) := \min_w \overleftarrow{J}(x, s; -b_-, w)$ , which is the minimum cost over all admissible values of  $w$ . It satisfies the *Dynamic Programming equation* [48, 49],

$$\partial_s \overleftarrow{W} + \frac{\sigma^2}{2} \nabla^2 \overleftarrow{W} - \nabla \cdot b_- = \min_w \left( -\frac{1}{2\sigma^2} \|b_- - w\|^2 - w \cdot \nabla \overleftarrow{W} \right). \quad (\text{B.12})$$

---

<sup>12</sup> $B'_s$  is a reparameterization of  $\hat{B}_s$ . See Sec. 4 of [8]



Pointwise minimization of the r.h.s. gives  $w_* = b_- - \sigma^2 \nabla \overleftarrow{W}$ . Substituting this back into Eq. (B.12) we find that  $\overleftarrow{W}$  solves

$$\partial_s \overleftarrow{W} + b_+ \cdot \nabla \overleftarrow{W} + \frac{\sigma^2}{2} \nabla^2 \overleftarrow{W} = \frac{\sigma^2}{2} \|\nabla \overleftarrow{W}\|^2 + \sigma^2 \nabla \log \overleftarrow{p} \cdot \nabla \overleftarrow{W} + \nabla \cdot b_-, \quad (\text{B.13})$$

with terminal value  $\overleftarrow{W}(x, T) = -\log p_0(x)$ . But notice that, for  $v = -b_-$ , Eq. (B.3) can be written as following equation for  $\overleftarrow{S} := -\log \overleftarrow{p}$ ,

$$\partial_s \overleftarrow{S} + b_+ \cdot \nabla \overleftarrow{S} + \frac{\sigma^2}{2} \nabla^2 \overleftarrow{S} = -\frac{\sigma^2}{2} \|\nabla \overleftarrow{S}\|^2 + \nabla \cdot b_-, \quad (\text{B.14})$$

also with a terminal value  $\overleftarrow{S}(x, T) = -\log p_0(x)$ . Comparing Eqs. (B.13) and (B.14), we see that  $\overleftarrow{W}(x, s) = -\log \overleftarrow{p}(x, s)$ , and Eq. (B.11) becomes

$$\begin{aligned} \log p(x, T) &= -\overleftarrow{W}(x, 0) \\ &= \mathbb{E}_{b_+} \left[ \int_s^T d\bar{s} \left( \frac{1}{2\sigma^2} \|\nabla \log \overleftarrow{p}\|^2 - \nabla \cdot b_- \right) - \log p_0(Y_T) \Big| Y_0 = x \right]. \end{aligned} \quad (\text{B.15})$$

The bound on the KL divergence between  $p$  and  $p_u$  can be obtained by integrating Eqs. (B.10) and (B.15) over  $p_d$ ,

$$-\int_0^T d\bar{s} \mathbb{E}_{\overleftarrow{p}} \left[ \frac{\|b_+ - b_-\|^2 - \|b_+ - u\|^2}{2\sigma^2} - \nabla \cdot (b_- - u) \right] \geq D_{KL}(p(\cdot, T) \| p_u(\cdot, T)). \quad (\text{B.16})$$

The last term in the average can be integrated by parts,

$$-\mathbb{E}_{\overleftarrow{p}} [\nabla \cdot (b_- - u)] = \mathbb{E}_{\overleftarrow{p}} [(b_- - u) \cdot \nabla \log \overleftarrow{p}] \stackrel{(2.3)}{=} \frac{1}{\sigma^2} \mathbb{E}_{\overleftarrow{p}} [(b_- - u) \cdot (b_- - b_+)], \quad (\text{B.17})$$

to rewrite Eq. (B.16) in its final form

$$\int_0^T d\bar{s} \frac{1}{2\sigma^2} \mathbb{E}_{\overleftarrow{p}} [\|b_- - u\|^2] \geq D_{KL}(p(\cdot, T) \| p_u(\cdot, T)). \quad (\text{B.18})$$

Note that (a) since  $p(\cdot, t) = \overleftarrow{p}(\cdot, s)$  we can replace the average  $\mathbb{E}_{\overleftarrow{p}} \rightarrow \mathbb{E}_p$  and change the time integral to run over  $t$ , which gives Eq. (2.5), and (b) we would have an additional KL term if we had  $p_v(\cdot, 0) \neq p_u(\cdot, 0)$  in Eq. (B.16), the one from Eq. (2.6).

## B.2 The $H$ -theorem

We derive Eq. (3.5) here, following [15]. It states that  $p$  relaxes toward  $p^{\text{eq}}$ , with the rate of approach slowing down as it nears that state. To prove it we start with the time derivative

$$\begin{aligned}
& -\frac{d}{dt} D_{KL}(p(x, t) || p_t^{\text{eq}}(x)) \\
&= \frac{d}{dt} \mathbb{E}_p \left[ -\log \frac{p(x, t)}{p_t^{\text{eq}}(x)} \right] \\
&= \frac{d}{dt} \left( -\int dx p(x, t) \log p(x, t) \right) - \frac{d}{dt} \left( -\int dx p(x, t) \log p_t^{\text{eq}}(x) \right). \quad (\text{B.19})
\end{aligned}$$

The first term on the r.h.s. is the Gibbs entropy production rate  $\dot{S}(t)$ ,

$$\begin{aligned}
\dot{S}(t) &= -\int dx \partial_t p \log p - \int dx \partial_t p \\
&= \int dx \left( -\nabla \cdot (b_- p) - \frac{\sigma^2}{2} \nabla^2 p \right) \log p + \int dx \nabla(\dots) \\
&\stackrel{\text{IBP}}{=} \int dx p(x, t) \left( \frac{\sigma^2}{2} \|\nabla \log p\|^2 + b_- \cdot \nabla \log p \right). \quad (\text{B.20})
\end{aligned}$$

The second term in Eq. (B.19) can be simplified by using the Fokker-Plack equations for  $p$  and  $p^{\text{eq}}$ ,

$$\begin{aligned}
& \frac{d}{dt} \left( \int dx p(x, t) \log p_t^{\text{eq}}(x) \right) \\
&= \int dx \left( \partial_t p(x, t) \log p_t^{\text{eq}}(x) + p(x, t) \frac{\partial_t p_t^{\text{eq}}(x)}{p_t^{\text{eq}}(x)} \right) \\
&= \int dx \left( \nabla \cdot (b_- p) + \frac{\sigma^2}{2} \nabla^2 p \right) \log p_t^{\text{eq}}(x) + \int dx \frac{p(x, t)}{p_t^{\text{eq}}(x)} \left( -\nabla \cdot (b_+ p_t^{\text{eq}}) + \frac{\sigma^2}{2} \nabla^2 p_t^{\text{eq}} \right).
\end{aligned}$$

We will consider each new term separately for clarity. Integrating by parts,

$$\begin{aligned}
& \int dx \left( \nabla \cdot (b_- p) + \frac{\sigma^2}{2} \nabla^2 p \right) \log p_t^{\text{eq}}(x) \\
&= \int dx p(x, t) \left( -b_- \cdot \nabla \log p_t^{\text{eq}} - \frac{\sigma^2}{2} \nabla \log p \cdot \nabla \log p_t^{\text{eq}} \right),
\end{aligned}$$

and

$$\begin{aligned}
& \int dx \frac{p(x, t)}{p_t^{\text{eq}}(x)} \left( -\nabla \cdot (b_+ p_t^{\text{eq}}) + \frac{\sigma^2}{2} \nabla^2 p_t^{\text{eq}} \right) \\
&= \int dx \left( b_+ \cdot \nabla p - b_+ p \cdot \frac{\nabla p_t^{\text{eq}}}{p_t^{\text{eq}}} - \frac{\sigma^2}{2} \nabla \log p \cdot \nabla \log p_t^{\text{eq}} + \frac{\sigma^2}{2} p \|\nabla \log p_t^{\text{eq}}\|^2 \right), \\
&= \int dx p(x, t) \left( b_+ \cdot (\nabla \log p - \nabla \log p_t^{\text{eq}}) - \frac{\sigma^2}{2} \nabla \log p \cdot \nabla \log p_t^{\text{eq}} + \frac{\sigma^2}{2} \|\nabla \log p_t^{\text{eq}}\|^2 \right).
\end{aligned}$$

Adding up everything, we obtain

$$\begin{aligned}
& -\frac{d}{dt} D_{KL}(p(x, t) \| p_t^{\text{eq}}(x)) \\
&= \mathbb{E}_p \left[ \frac{\sigma^2}{2} \|\nabla \log p(x, t) - \nabla \log p_t^{\text{eq}}(x)\|^2 + (b_- + b_+) \cdot (\nabla \log p(x, t) - \nabla \log p_t^{\text{eq}}(x)) \right] \\
&= -\mathbb{E}_p \left[ \frac{1}{2\sigma^2} \|2b_+ - \sigma^2 \nabla \log p(x, t)\|^2 \right], \tag{B.21}
\end{aligned}$$

where in the last step we used Eq. (3.4) to replace  $\nabla \log p_t^{\text{eq}}(x)$ . Integrating Eq. (B.21) yields Eq. (3.5).

### B.3 Denoising Objective

We want to train a diffusion model to minimize the explicit entropy matching objective (EEM) (cf. Eq. (6.3))<sup>13</sup>

$$\int_0^T ds \sigma^2 \mathbb{E}_{Y_s} \left[ \frac{1}{2} \left\| \frac{2b_+}{\sigma^2} - \nabla \log \overleftarrow{p} + \mathbf{e}_\theta \right\|^2 \right] =: \int_0^T ds \sigma^2 \mathcal{L}_{\text{EEM}}, \tag{B.22}$$

Since we do not know the actual score function  $\nabla \log \overleftarrow{p}$  we convert this to the denoising entropy matching form, following [50]. Defining  $\mathbf{h}_\theta := 2b_+/\sigma^2 + \mathbf{e}_\theta$ , we expand

$$\begin{aligned}
\mathcal{L}_{\text{EEM}} &= \mathbb{E}_{Y_s} \left[ \frac{1}{2} \left\| \mathbf{h}_\theta(Y_s, s) - \nabla \log \overleftarrow{p}(Y_s, s) \right\|^2 \right] \\
&= \mathbb{E}_{Y_s} \left[ \frac{1}{2} \|\mathbf{h}_\theta(Y_s, s)\|^2 - \mathbf{h}_\theta(Y_s, s) \cdot \nabla \log \overleftarrow{p}(Y_s, s) + \frac{1}{2} \left\| \nabla \log \overleftarrow{p}(Y_s, s) \right\|^2 \right].
\end{aligned}$$

The cross term can be written as

---

<sup>13</sup> $\mathbb{E}_{Y_s}$  is the same as  $\mathbb{E}_{\overleftarrow{p}}$  or  $\mathbb{E}_p$ ; we use this notation to contrast with  $\mathbb{E}_{Y_s, Y_0}$  in Eq. (B.24).

$$\begin{aligned}
\mathbb{E}_{Y_s} \left[ \mathbf{h}_\theta(Y_s, s) \cdot \nabla \log \overleftarrow{p}(Y_s, s) \right] &\stackrel{\text{IBP}}{=} \int dy_s \mathbf{h}_\theta(y_s, s) \cdot \nabla p(y, s) \\
&= \int dy_s \mathbf{h}_\theta(y_s, s) \cdot \nabla \int dy_0 \overleftarrow{p}(y_s|y_0) \overleftarrow{p}(y_0, 0) \\
&= \int dy_s \int dy_0 \overleftarrow{p}(y_0, 0) \overleftarrow{p}(y_s|y_0) \mathbf{h}_\theta(y_s, s) \cdot \nabla \log \overleftarrow{p}(y_s|y_0) \\
&= \mathbb{E}_{Y_s, Y_0} \left[ \mathbf{h}_\theta(Y_s, s) \cdot \nabla \log \overleftarrow{p}(Y_s|Y_0) \right],
\end{aligned}$$

where  $\overleftarrow{p}(y_s|y_0)$  is the transition probability of arriving at  $y_s$  starting from  $y_0$ , under Eq. (2.1). The expectation value in the final step is taken over the joint density  $\overleftarrow{p}(y_s, y_0)$ . Then,

$$\begin{aligned}
\mathcal{L}_{\text{EEM}} - \frac{1}{2} \mathbb{E}_{Y_s} \left[ \left\| \nabla \log \overleftarrow{p}(Y_s, s) \right\|^2 \right] & \tag{B.23} \\
&= \mathbb{E}_{Y_s, Y_0} \left[ \frac{1}{2} \left\| \mathbf{h}_\theta(Y_s, s) \right\|^2 - \mathbf{h}_\theta(Y_s, s) \cdot \nabla \log \overleftarrow{p}(y_s|y_0) \right] \\
&= \mathbb{E}_{Y_s, Y_0} \left[ \frac{1}{2} \left\| \mathbf{h}_\theta(Y_s, s) - \nabla \log \overleftarrow{p}(Y_s|Y_0) \right\|^2 \right] - \frac{1}{2} \mathbb{E}_{Y_s, Y_0} \left[ \left\| \nabla \log \overleftarrow{p}(Y_s|Y_0) \right\|^2 \right],
\end{aligned} \tag{B.24}$$

from which we identify the denoising entropy matching term, the only piece that involves the network  $\mathbf{h}_\theta$ ,

$$\mathcal{L}_{\text{DEM}} := \mathbb{E}_{Y_s, Y_0} \left[ \frac{1}{2} \left\| \mathbf{h}_\theta(Y_s, s) - \nabla \log \overleftarrow{p}(Y_s|Y_0) \right\|^2 \right]. \tag{B.25}$$

Since  $\mathcal{L}_{\text{EEM}}$  and  $\mathcal{L}_{\text{DEM}}$  differ only by terms that do not depend on  $\theta$ , replacing the former with the latter in Eq. (B.22) gives an equivalent training objective,

$$\int_0^T ds \sigma^2 \mathbb{E}_{Y_s, Y_0} \left[ \frac{1}{2} \left\| \frac{2b_+}{\sigma^2} - \nabla \log \overleftarrow{p}(Y_s|Y_0) + \mathbf{e}_\theta \right\|^2 \right]. \tag{B.26}$$

Some intuition for this expression is given in Sec. 4.3 of [24]. The time integral and expectation values can be estimated by Monte Carlo [5],

$$\mathbb{E}_{s \sim \mathcal{U}(0, T)} \left[ \sigma(s)^2 \mathbb{E}_{y_0 \sim p_d(y_0)} \mathbb{E}_{y_s \sim \overleftarrow{p}(y_s|y_0)} \left[ \frac{1}{2} \left\| \frac{2b_+}{\sigma^2} - \nabla \log \overleftarrow{p}(y_s|y_0) + \mathbf{e}_\theta \right\|^2 \right] \right]. \tag{B.27}$$

The time variable  $s$  is sampled uniformly in the interval  $(0, T]$ . The data vectors from  $\overleftarrow{p}(y_0, 0) \equiv p_d(y_0)$  can be propagated to  $s$  efficiently if we have a closed-form expression for the kernel  $\overleftarrow{p}(y_s|y_0)$ . For a driftless diffusion process (VE) or an Ornstein-Uhlenbeck process (VP) the kernel is a Gaussian, which allows us to (a) sample the objective in Eq. (6.4) without solving the SDE Eq. (2.1), and (b) compute  $\overleftarrow{p}(y_s|y_0)$  for finite  $s$ .

Following [9] we also introduce a weighting function  $\lambda(s)$  that can be adjusted to switch between maximum likelihood training and the ELBO [6]. Then, the actual loss function is

$$\mathbb{E}_{s \sim \mathcal{U}(0, T)} \left[ \lambda(s) \sigma(s)^2 \mathbb{E}_{y_0 \sim p_d(y_0)} \mathbb{E}_{y_s \sim \overleftarrow{p}(y_s|y_0)} \left[ \frac{1}{2} \left\| \frac{2b_+}{\sigma^2} - \nabla \log \overleftarrow{p}(y_s|y_0) + \mathbf{e}_\theta \right\|^2 \right] \right], \quad (\text{B.28})$$

where

$$\lambda(s) = \begin{cases} 1, & \text{maximum likelihood,} \\ \frac{2\Sigma(s)^2}{\sigma(s)^2}, & \text{ELBO.} \end{cases} \quad (\text{B.29})$$

Here  $\Sigma(s)^2$  is the variance of the (Gaussian) kernel  $\overleftarrow{p}(y_s|y_0)$ . The ELBO choice softens the divergent behavior of  $\nabla \log \overleftarrow{p}(y_s|y_0) \sim \Sigma(s)^{-1}$  near  $s = 0$ , and leads to a smoother convergence of the loss in Eq. (B.28). Empirically, we also find that it gives better results for the KL between original data distribution and the generated one. On the other hand, the maximum likelihood option produces large fluctuations in the loss function, and a worse KL. Importance sampling is suggested as a remedy to this problem in [9], however we did not implement this in our experiments because of differences in how we train our model. The ELBO loss was used for all the results in Sec. 7.

## References

- [1] L. Boltzmann, *Further Studies on the Thermal Equilibrium of Gas Molecules*, pp. 262–349. 2003.
- [2] C. E. Shannon, “A mathematical theory of communication,” *The Bell System Technical Journal* **27** no. 3, (1948) 379–423.
- [3] J. C. Maxwell, “Life and scientific work of peter guthrie tait,” in *Life and Scientific Work of Peter Guthrie Tait*, C. G. Knott, ed., p. 213. Cambridge University Press, London, 1911.
- [4] J. Sohl-Dickstein, E. Weiss, N. Maheswaranathan, and S. Ganguli, “Deep unsupervised learning using nonequilibrium thermodynamics,” in *Proceedings of the 32nd International Conference on Machine Learning*, F. Bach and D. Blei, eds., vol. 37 of *Proceedings of Machine Learning Research*, pp. 2256–2265. PMLR, Lille, France, 07–09 jul, 2015. <https://proceedings.mlr.press/v37/sohl-dickstein15.html>.
- [5] Y. Song, J. Sohl-Dickstein, D. P. Kingma, A. Kumar, S. Ermon, and B. Poole, “Score-based generative modeling through stochastic differential equations,” in *9th International Conference on Learning Representations, ICLR 2021, Virtual Event, Austria, May 3-7, 2021*. OpenReview.net, 2021. <https://openreview.net/forum?id=PXTIG12RRHS>.
- [6] J. Ho, A. Jain, and P. Abbeel, “Denoising diffusion probabilistic models,” in *Advances in Neural Information Processing Systems 33: Annual Conference on Neural Information Processing Systems 2020, NeurIPS 2020, December 6-12, 2020, virtual*, H. Larochelle, M. Ranzato, R. Hadsell, M. Balcan, and H. Lin, eds. 2020. <https://proceedings.neurips.cc/paper/2020/hash/4c5bcfec8584af0d967f1ab10179ca4b-Abstract.html>.
- [7] J.-D. Benamou and Y. Brenier, “A computational fluid mechanics solution to the monge-kantorovich mass transfer problem,” *Numerische Mathematik* **84** no. 3, (Jan, 2000) 375–393. <https://doi.org/10.1007/s002110050002>.
- [8] C.-W. Huang, J. H. Lim, and A. C. Courville, “A variational perspective on diffusion-based generative models and score matching,” in *Advances in Neural Information Processing Systems*, M. Ranzato, A. Beygelzimer, Y. Dauphin, P. Liang, and J. W. Vaughan, eds., vol. 34, pp. 22863–22876. Curran Associates, Inc., 2021. [https://proceedings.neurips.cc/paper\\_files/paper/2021/file/c11abfd29e4d9b4d4b566b01114d8486-Paper.pdf](https://proceedings.neurips.cc/paper_files/paper/2021/file/c11abfd29e4d9b4d4b566b01114d8486-Paper.pdf).
- [9] Y. Song, C. Durkan, I. Murray, and S. Ermon, “Maximum likelihood training of score-based diffusion models,” in *Advances in Neural Information Processing Systems*, M. Ranzato, A. Beygelzimer, Y. Dauphin, P. Liang, and J. W. Vaughan, eds., vol. 34,

- pp. 1415–1428. Curran Associates, Inc., 2021. [https://proceedings.neurips.cc/paper\\_files/paper/2021/file/0a9fdbb17feb6ccb7ec405cfb85222c4-Paper.pdf](https://proceedings.neurips.cc/paper_files/paper/2021/file/0a9fdbb17feb6ccb7ec405cfb85222c4-Paper.pdf).
- [10] E. Nelson, “Derivation of the schrödinger equation from newtonian mechanics,” *Phys. Rev.* **150** (Oct, 1966) 1079–1085.  
<https://link.aps.org/doi/10.1103/PhysRev.150.1079>.
- [11] B. D. Anderson, “Reverse-time diffusion equation models,” *Stochastic Processes and their Applications* **12** no. 3, (1982) 313–326.  
<https://www.sciencedirect.com/science/article/pii/0304414982900515>.
- [12] U. G. Haussmann and E. Pardoux, “Time Reversal of Diffusions,” *The Annals of Probability* **14** no. 4, (1986) 1188 – 1205. <https://doi.org/10.1214/aop/1176992362>.
- [13] H. Föllmer, “Random fields and diffusion processes,” in *École d’Été de Probabilités de Saint-Flour XV–XVII, 1985–87*, P.-L. Hennequin, ed., pp. 101–203. Springer Berlin Heidelberg, Berlin, Heidelberg, 1988.
- [14] U. Seifert, “Stochastic thermodynamics, fluctuation theorems and molecular machines,” *Reports on Progress in Physics* **75** no. 12, (Nov, 2012) 126001.  
<https://dx.doi.org/10.1088/0034-4885/75/12/126001>.
- [15] M. Pavon, “Stochastic control and nonequilibrium thermodynamical systems,” *Applied Mathematics and Optimization* **19** no. 1, (1989) 187–202.  
<https://doi.org/10.1007/BF01448198>.
- [16] H. Ge and D.-Q. Jiang, “Generalized jarzynski’s equality of inhomogeneous multidimensional diffusion processes,” *Journal of Statistical Physics* **131** no. 4, (5, 2008) 675–689. <https://doi.org/10.1007/s10955-008-9520-4>.
- [17] C. Jarzynski, “Rare events and the convergence of exponentially averaged work values,” *Phys. Rev. E* **73** (Apr, 2006) 046105.  
<https://link.aps.org/doi/10.1103/PhysRevE.73.046105>.
- [18] J. M. R. Parrondo, C. V. den Broeck, and R. Kawai, “Entropy production and the arrow of time,” *New Journal of Physics* **11** no. 7, (Jul, 2009) 073008.  
<https://dx.doi.org/10.1088/1367-2630/11/7/073008>.
- [19] U. Seifert, “Entropy production along a stochastic trajectory and an integral fluctuation theorem,” *Phys. Rev. Lett.* **95** (Jul, 2005) 040602.  
<https://link.aps.org/doi/10.1103/PhysRevLett.95.040602>.
- [20] S. Vaikuntanathan and C. Jarzynski, “Dissipation and lag in irreversible processes,” *Europhysics Letters* **87** no. 6, (Oct, 2009) 60005.  
<https://dx.doi.org/10.1209/0295-5075/87/60005>.

- [21] E. T. Jaynes, “Information theory and statistical mechanics,” *Phys. Rev.* **106** (May, 1957) 620–630. <https://link.aps.org/doi/10.1103/PhysRev.106.620>.
- [22] E. T. Jaynes, “Gibbs vs Boltzmann Entropies,” *American Journal of Physics* **33** no. 5, (05, 1965) 391–398, [https://pubs.aip.org/aapt/ajp/article-pdf/33/5/391/12040108/391\\_1\\_online.pdf](https://pubs.aip.org/aapt/ajp/article-pdf/33/5/391/12040108/391_1_online.pdf). <https://doi.org/10.1119/1.1971557>.
- [23] R. Chetrite, P. Muratore-Ginanneschi, and K. Schwieger, “E. schrödinger’s 1931 paper “on the reversal of the laws of nature” [“über die umkehrung der naturgesetze”, sitzungsberichte der preussischen akademie der wissenschaften, physikalisch-mathematische klasse, 8 n9 144–153],” *The European Physical Journal H* **46** no. 1, (Nov, 2021) 28. <https://doi.org/10.1140/epjh/s13129-021-00032-7>.
- [24] A. Premkumar, “Generative diffusion from an action principle,” 2023. <https://arxiv.org/abs/2310.04490>.
- [25] C. Jarzynski, “Equilibrium free-energy differences from nonequilibrium measurements: A master-equation approach,” *Phys. Rev. E* **56** (Nov, 1997) 5018–5035. <https://link.aps.org/doi/10.1103/PhysRevE.56.5018>.
- [26] G. E. Crooks and C. Jarzynski, “Work distribution for the adiabatic compression of a dilute and interacting classical gas,” *Phys. Rev. E* **75** (Feb, 2007) 021116. <https://link.aps.org/doi/10.1103/PhysRevE.75.021116>.
- [27] C. Jarzynski, *Equalities and Inequalities: Irreversibility and the Second Law of Thermodynamics at the Nanoscale*, pp. 145–172. Springer Basel, Basel, 2013. [https://doi.org/10.1007/978-3-0348-0359-5\\_4](https://doi.org/10.1007/978-3-0348-0359-5_4).
- [28] E. T. Jaynes, “Information theory and statistical mechanics. ii,” *Phys. Rev.* **108** (Oct, 1957) 171–190. <https://link.aps.org/doi/10.1103/PhysRev.108.171>.
- [29] K. Maruyama, F. Nori, and V. Vedral, “Colloquium: The physics of maxwell’s demon and information,” *Rev. Mod. Phys.* **81** (Jan, 2009) 1–23. <https://link.aps.org/doi/10.1103/RevModPhys.81.1>.
- [30] R. Landauer, “Irreversibility and heat generation in the computing process,” *IBM Journal of Research and Development* **5** no. 3, (1961) 183–191.
- [31] O. Penrose, “Foundations of statistical mechanics,” *Reports on Progress in Physics* **42** no. 12, (Dec, 1979) 1937. <https://dx.doi.org/10.1088/0034-4885/42/12/002>.
- [32] C. H. Bennett, “The thermodynamics of computation—a review,” *International Journal of Theoretical Physics* **21** no. 12, (1982) 905–940. <https://doi.org/10.1007/BF02084158>.



- [33] T. Van Vu and K. Saito, “Thermodynamic unification of optimal transport: Thermodynamic uncertainty relation, minimum dissipation, and thermodynamic speed limits,” *Phys. Rev. X* **13** (Feb, 2023) 011013. <https://link.aps.org/doi/10.1103/PhysRevX.13.011013>.
- [34] D. Kwon, Y. Fan, and K. Lee, “Score-based generative modeling secretly minimizes the wasserstein distance,” *CoRR* [abs/2212.06359](https://arxiv.org/abs/2212.06359) (2022) , 2212.06359. <https://doi.org/10.48550/arXiv.2212.06359>.
- [35] K. Ikeda, T. Uda, D. Okanojara, and S. Ito, “Speed-accuracy trade-off for the diffusion models: Wisdom from nonequilibrium thermodynamics and optimal transport,” 2024. <https://arxiv.org/abs/2407.04495>.
- [36] M. Tancik, P. Srinivasan, B. Mildenhall, S. Fridovich-Keil, N. Raghavan, U. Singhal, R. Ramamoorthi, J. Barron, and R. Ng, “Fourier features let networks learn high frequency functions in low dimensional domains,” in *Advances in Neural Information Processing Systems*, H. Larochelle, M. Ranzato, R. Hadsell, M. Balcan, and H. Lin, eds., vol. 33, pp. 7537–7547. Curran Associates, Inc., 2020. [https://proceedings.neurips.cc/paper\\_files/paper/2020/file/55053683268957697aa39fba6f231c68-Paper.pdf](https://proceedings.neurips.cc/paper_files/paper/2020/file/55053683268957697aa39fba6f231c68-Paper.pdf).
- [37] W. Peebles and S. Xie, “Scalable diffusion models with transformers,” in *Proceedings of the IEEE/CVF International Conference on Computer Vision (ICCV)*, pp. 4195–4205. October, 2023.
- [38] Q. Zhang and Y. Chen, “Path integral sampler: a stochastic control approach for sampling,” in *International Conference on Learning Representations*. 2022.
- [39] J. Berner, L. Richter, and K. Ullrich, “An optimal control perspective on diffusion-based generative modeling,” *Transactions on Machine Learning Research* (2024) . <https://openreview.net/forum?id=oYIjw37pTP>.
- [40] R. Chetrite and K. Gawędzki, “Fluctuation relations for diffusion processes,” *Communications in Mathematical Physics* **282** no. 2, (2008) 469–518. <https://doi.org/10.1007/s00220-008-0502-9>.
- [41] G. E. Crooks, “Nonequilibrium measurements of free energy differences for microscopically reversible markovian systems,” *Journal of Statistical Physics* **90** no. 5, (1998) 1481–1487. <https://doi.org/10.1023/A:1023208217925>.
- [42] R. Kawai, J. M. R. Parrondo, and C. V. den Broeck, “Dissipation: The phase-space perspective,” *Phys. Rev. Lett.* **98** (Feb, 2007) 080602. <https://link.aps.org/doi/10.1103/PhysRevLett.98.080602>.
- [43] T. Cohen, D. Green, and A. Premkumar, “A tail of eternal inflation,” *SciPost Phys.* **14** (2023) 109. <https://scipost.org/10.21468/SciPostPhys.14.5.109>.

- [44] T. Cohen, D. Green, and A. Premkumar, “Large deviations in the early universe,” *Phys. Rev. D* **107** (Apr, 2023) 083501.  
<https://link.aps.org/doi/10.1103/PhysRevD.107.083501>.
- [45] J. Cotler and S. Rezchikov, “Renormalization group flow as optimal transport,” *Phys. Rev. D* **108** (Jul, 2023) 025003.  
<https://link.aps.org/doi/10.1103/PhysRevD.108.025003>.
- [46] D. S. Berman, M. S. Klinger, and A. G. Stapleton, “Bayesian renormalization,” *Machine Learning: Science and Technology* **4** no. 4, (Oct, 2023) 045011.  
<https://dx.doi.org/10.1088/2632-2153/ad0102>.
- [47] T. M. Cover and J. A. Thomas, *Elements of Information Theory (Wiley Series in Telecommunications and Signal Processing)*. Wiley-Interscience, USA, 2006.
- [48] W. Fleming and R. Rishel, *Deterministic and Stochastic Optimal Control*. Stochastic Modelling and Applied Probability. Springer New York, NY, 1 ed., 1975.  
<https://doi.org/10.1007/978-1-4612-6380-7>.
- [49] M. Kamien and N. Schwartz, *Dynamic Optimization, Second Edition: The Calculus of Variations and Optimal Control in Economics and Management*. Dover Books on Mathematics. Dover Publications, 2013.  
<https://books.google.com/books?id=liLCAgAAQBAJ>.
- [50] P. Vincent, “A connection between score matching and denoising autoencoders,” *Neural Computation* **23** (2011) 1661–1674.  
<https://api.semanticscholar.org/CorpusID:5560643>.